A Conserved Long Noncoding RNA Affects Sleep Behavior in *Drosophila*

Alexey A. Soshnev,* Hiroshi Ishimoto,† Bryant F. McAllister,‡ Xingguo Li,§,1 Misty D. Wehling,§ Toshihiro Kitamoto,† and Pamela K. Geyer*,§,2

*Program in Molecular and Cellular Biology, †Department of Anesthesia, ‡Department of Biology, and §Department of Biochemistry, University of Iowa, Iowa City, Iowa 52242

ABSTRACT Metazoan genomes encode an abundant collection of mRNA-like, long noncoding (lnc)RNAs. Although lncRNAs greatly expand the transcriptional repertoire, we have a limited understanding of how these RNAs contribute to developmental regulation. Here, we investigate the function of the *Drosophila* lncRNA called ***y**ellow-**a**chaete intergenic **R**NA* (*yar*). Comparative sequence analyses show that the *yar* gene is conserved in *Drosophila* species representing 40–60 million years of evolution, with one of the conserved sequence motifs encompassing the *yar* promoter. Further, the timing of *yar* expression in *Drosophila virilis* parallels that in *D. melanogaster*, suggesting that transcriptional regulation of *yar* is conserved. The function of *yar* was defined by generating null alleles. Flies lacking *yar* RNAs are viable and show no overt morphological defects, consistent with maintained transcriptional regulation of the adjacent *yellow* (*y*) and *achaete* (*ac*) genes. The location of *yar* within a neural gene cluster led to the investigation of effects of *yar* in behavioral assays. These studies demonstrated that loss of *yar* alters sleep regulation in the context of a normal circadian rhythm. Nighttime sleep was reduced and fragmented, with *yar* mutants displaying diminished sleep rebound following sleep deprivation. Importantly, these defects were rescued by a *yar* transgene. These data provide the first example of a lncRNA gene involved in *Drosophila* sleep regulation. We find that *yar* is a cytoplasmic lncRNA, suggesting that *yar* may regulate sleep by affecting stabilization or translational regulation of mRNAs. Such functions of lncRNAs may extend to vertebrates, as lncRNAs are abundant in neural tissues.

METAZOAN genomes encode an abundant collection of noncoding (nc) RNAs. These include housekeeping ncRNAs, such as transfer RNAs and ribosomal RNAs, and a growing number of regulatory ncRNAs. Regulatory ncRNAs have been categorized into two subclasses, on the basis of length (Prasanth and Spector 2007; Mercer *et al.* 2009). RNAs <200 nucleotides encompass the small ncRNAs class, which includes endogenous small interfering (endo si) RNAs, micro (mi) RNAs and piwi-interacting (pi) RNAs. RNAs >200 nucleotides encompass the long ncRNA (lncRNA) class. Many lncRNAs share properties with mRNAs, being transcribed by RNA polymerase II and processed by the splicing and polyadenylation machinery. Emerging evidence indicates that regulatory RNAs make multiple contributions to cellular functions (Mercer *et al.* 2009; Chen and Carmichael 2010; Taft *et al.* 2010; Clark and Mattick 2011). Small ncRNAs function primarily in the cytoplasm, working as guides for the recognition of regulated target RNAs by associated protein complexes. LncRNAs localize both to the nucleus and cytoplasm. Nuclear lncRNAs have many regulatory roles, including organization of nuclear architecture and control of transcription, splicing, and nuclear trafficking (Mercer *et al.* 2009; Chen and Carmichael 2010; Taft *et al.* 2010; Clark and Mattick 2011). Recently, cytoplasmic roles for lncRNAs have been uncovered, including regulation of mRNA decay and miRNA function (Panzitt *et al.* 2007; Matouk *et al.* 2009; Wang *et al.* 2010; Clark and Mattick 2011). These observations demonstrate that regulatory RNAs expand the functional repertoire of the transcriptome in developing organisms.

The *Drosophila melanogaster* genome has been estimated to encode >100 lncRNAs (Tupy *et al.* 2005; Willingham *et al.* 2006; Graveley *et al.* 2011). Many of these lncRNA genes are transcribed during embryogenesis and display spatially

doi: 10.1534/genetics.111.131706
Manuscript received June 15, 2011; accepted for publication July 16, 2011
Available freely online through the author-supported open access option.
Supporting information is available online at http://www.genetics.org/content/suppl/2011/07/20/genetics.111.131706.DC1.
[1]Present address: Department of Biochemistry and Molecular Biology, University of Florida, FL 32610.
[2]Corresponding author: Department of Biochemistry, 3135E MERF, University of Iowa, Iowa City, IA 52242. E-mail: pamela-geyer@uiowa.edu

restricted expression, with predominant RNA accumulation in the developing central and peripheral nervous system (Inagaki *et al.* 2005; Li *et al.* 2009). While many *Drosophila* lncRNAs have been identified, mutations in only a small number of these genes are known and are limited to genes encoding nuclear lncRNAs. Two lncRNA genes that have been studied genetically encode the nuclear retained *roX1* and *roX2* RNAs, essential RNAs involved in dosage compensation (Meller and Rattner 2002; Deng and Meller 2006). Although the *roX* RNAs display limited sequence identity, these RNAs share a role in assembly and targeting of the dosage compensation complex to the male *X* chromosome (Ilik and Akhtar 2009; Koya and Meller 2011). A third genetically studied *Drosophila* lncRNA gene is *hsr-ω* gene, which encodes the heat inducible *hsr-ω-n* transcript (Jolly and Lakhotia 2006). This essential gene encodes a large, nuclear retained lncRNA, which forms nucleoplasmic omega speckles that accumulate heterogeneous nuclear RNA binding proteins (hnRNPs) (Prasanth *et al.* 2000). Recent evidence suggests that *hsr-ω-n* functions as a hub for coordination of transcriptional regulators and hnRNPs, impacting cellular responses such as apoptosis (Mallik and Lakhotia 2010). While our understanding of the *in vivo* functions of lncRNAs remains limited, the essential roles of these three nuclear-retained lncRNAs suggest that lncRNAs make multiple contributions to development and cell differentiation.

The *Drosophila* ***y****ellow-****a****chaete* (*ac*) *intergenic* ***R****NA* (*yar*) is a newly identified lncRNA gene. This gene encodes multiple alternatively spliced poly(A)$^+$ RNAs that are highly expressed during midembryogenesis. As *yar* RNAs lack a predicted translation product >75 amino acids, *yar* has been classified as a lncRNA gene. Within the *Drosophila* genome, *yar* resides within a neural gene cluster (Soshnev *et al.* 2008). Upstream of *yar* is *yellow* (*y*), a gene that encodes a secreted protein required for cuticle coloration and male sexual behavior (Nash and Yarkin 1974; Biessmann 1985; Chia *et al.* 1986; Geyer *et al.* 1986; Geyer and Corces 1987; Drapeau *et al.* 2003). Downstream of *yar* is *achaete* (*ac*), a gene that encodes one of four related bHLH transcription factors of the *achaete–scute* complex (AS-C) required for proper development of the central and peripheral nervous systems (Modolell and Campuzano 1998; Gibert and Simpson 2003; Negre and Simpson 2009). The order and transcriptional orientation of genes in the AS-C complex is remarkably conserved among insect species, and this organization extends to the *y* gene in most species (Negre and Simpson 2009). This linkage cannot be explained by shared enhancers, as *y*, *yar*, and *ac* show distinct temporal patterns of embryonic gene expression (Campuzano *et al.* 1985; Chia *et al.* 1986; Soshnev *et al.* 2008). Interestingly, transcription of *yar* coincides with down-regulation of the *ac* gene, while transcription of *y* coincides with down-regulation of *yar* (Soshnev *et al.* 2008). These observations suggest that temporal regulation of *y*, *yar*, and *ac* might be linked, a possibility supported by previously identified regulatory contributions of other ncRNA genes (Ogawa and Lee 2002; Martens *et al.* 2004; Petruk *et al.* 2006; Martianov *et al.* 2007).

Here, we use genomic and genetic approaches to define the role of *yar* in the *y–yar–ac* region. Genomic analyses revealed the presence of large blocks of sequence identity within *yar* that have been conserved over 40–60 million years of evolution. This conservation does not extend to the putative open reading frames within *yar* RNAs, supporting that *yar* is a lncRNA gene. Interestingly, the second largest block of sequence identity encompasses the three *yar* promoters (Soshnev *et al.* 2008). This conservation is reflected in the parallel temporal pattern of embryonic *yar* expression in the distantly related *D. melanogaster* and *D. virilis* species. We show that the *D. melanogaster yar* gene is globally expressed during midembryogenesis, with *yar* RNA accumulating in the cytoplasm. Using homologous recombination, two null alleles were generated. Flies lacking *yar* RNAs are viable and appropriately regulate *y* and *ac* transcription, but show defects in sleep. We uncovered that *yar* mutants exhibit shortened sleep bouts within a normal circadian sleep–wake cycle and have diminished levels of sleep rebound following deprivation. Importantly, both phenotypes are rescued by a transgene encompassing the *yar* gene, demonstrating that *yar* is required for sleep regulation. As *yar* is a cytoplasmic RNA, its regulatory effects are likely to depend upon stabilization or translational regulation of target RNAs. Our findings represent the first example of a lncRNA gene involved in *Drosophila* sleep behavior.

Materials and Methods

Fly stocks and crosses

Flies were raised at 25°, 70% humidity on standard cornmeal/agar medium. Description of the alleles used can be found at www.flybase.org.

Analyses of the y–ac intergenic region

Genomic sequences of the *y–ac* intergenic region from eight species of *Drosophila* were compared with *D. melanogaster*, including species in the subgenus *Sophophora* estimated to represent 10 million years (MY) of evolution (*D. yakuba* and *D. erecta*), and 20–30 MY (*D. ananassae*, *D. pseudoobscura*, and *D. willistoni*), and species in the subgenus *Drosophila* estimated to represent 40–60 MY of evolution (*D. virilis*, *D. mojavensis*, and *D. grimshawi*) (Stark *et al.* 2007). Sequences were obtained through FlyBase using Release 4 (www.flybase.org). Sequence alignments based on percentage of identity with nucleotide-level alignments were generated with MultiPipMaker (Schwartz *et al.* 2000). In all species except *D. mojavensis*, the *y* and *ac* genes are oriented the same as *D. melanogaster*, so sequence alignments were obtained with the corresponding intergenic interval. In *D. mojavensis*, *y* is not adjacent to *ac*. In this case, the "intergenic" regions were defined as an ~12-kb fragment either upstream of *ac* or downstream of *y*. Alignments in the genome of *D. mojavensis* revealed sequence

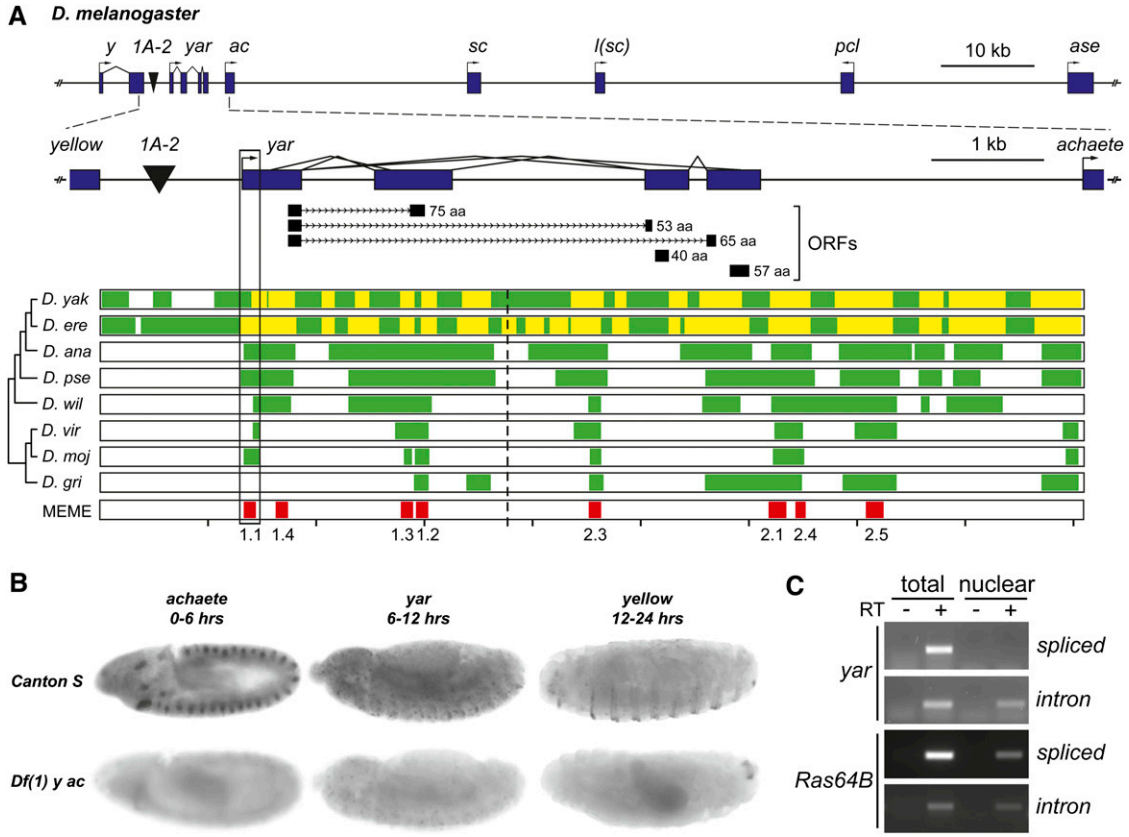

Figure 1 Conservation and tissue localization of *yar* RNA in *D. melanogaster*. (A) Multiple DNA motifs are conserved in the *y–ac* intergenic region. (A, top) Structure of the *D. melanogaster* genomic region that includes *y*, *yar*, the four AS-C genes, and *pepsinogen-like* (*pcl*). Genes are shown as rectangles, with promoters shown as bent arrows. The 1A-2 regulatory element is indicated by black inverted triangle. (A, middle) An expanded view of the 9-kb region separating *y* and *ac, including yar*, with a representation of its splicing pattern. The tracks located under the *yar* gene structure indicate the location of the potential *yar* ORFs, with the size of the peptide noted. (A, bottom) Aligned with the 9-kb region are the percentage of identity plots obtained from MultiPipMaker analyses of the corresponding regions from nine drosophilid species. Regions of no alignment are indicated in white, regions with significant BLASTZ alignment to *D. melanogaster* are indicated in green, and regions of nongapped alignments of >100 nucleotides with >70% identity are indicated in yellow. Conserved motifs identified by MEME are indicated on the bottom track. Motif 1.1 identifies the *yar* promoter. A gap in the genome sequence of *D. grimshawi* spans the region corresponding to motifs 1.1, 1.4, and 1.3. The dashed line indicates where the intergenic regions were split in two fragments for MEME analyses. (B) Whole mount RNA *in situ* hybridization of aged *D. melanogaster* embryos. *ac* mRNA is detected in the neuroectoderm clusters in the early embryogenesis, *yar* is globally expressed in midembryogenesis, and *y* is expressed in late embryogenesis in denticle belts. *Df(1) y ac* embryos serve as a negative control. (C) Analyses of cellular localization of *yar* transcripts. Total RNA isolated from equal amounts of unfractionated embryos and nuclear fraction was reverse transcribed and analyzed by semiquantitative PCR. The (−) RT lanes control for genomic DNA contamination. Spliced products were detected with primer pairs flanking the intron; intronic sequences were detected with primer pairs located within the intron. The housekeeping gene *Ras64B* serves as a positive control.

conservation in the upstream region of *ac* that includes *yar*. For this reason, all reported analyses only include the intergenic interval upstream of *ac*.

Nucleotide alignments revealed overall sequence conservation among nine *Drosophila* species and provided a guide for subdividing the intergenic region of each species into two approximately equal segments. Sequence motifs within each segment that were conserved across the nine species were identified using MEME (Figure 1) (Bailey *et al.* 2006). High-scoring sequence motifs were identified as regions of homology shared among the maximum set of species (a large gap is present in the genome sequence of segment 1 for *D. grimshawi*). These regions are likely to be constrained due to an evolutionarily conserved function. Each was given a unique identifier *x.y*, with *x* representing segment 1 or 2 and *y* representing the ordinal score in each MEME analysis. Each conserved MEME motif was mapped onto the sequence alignment of the *D. melanogaster* Release 5 (Figure 1, supporting information, Figure S1).

Analyses of y–ac intergenic transcription in D. virilis

Embryogenesis in *D. virilis* is prolonged relative to *D. melanogaster*, lasting 32 *vs.* 22 hr, respectively, after egg laying (Markow *et al.* 2009). RNA was isolated from aged *D. virilis* embryos as described previously (Parnell *et al.* 2006). This RNA was converted into cDNA using the HighCapacity cDNA kit (Applied Biosystems) with either random hexamers or oligo-dT primers for first strand synthesis. Primer pairs for PCR amplification of this cDNA were anchored within the MEME-identified conserved motifs or within the Genscan-predicted

exons of the intergenic transcript (Burge and Karlin 1997) (Figure 2, Figure S2, Table S1). As a control, all primer pairs were tested for amplification of *D. virilis* genomic DNA. In all cases, genomic DNA fragments of the appropriate size were obtained. Three independent RNA isolations were analyzed by PCR.

Whole mount in situ hybridization

Whole mount *in situ* hybridization on *Drosophila* embryos was performed as described previously (Tautz and Pfeifle 1989), with the overnight hybridization at 48°. Digoxigenin-labeled probes were generated from cDNAs encompassing the second exon of *y* (*Eco*RI–*Bgl*II fragment), first, third, and fourth exon of *yar* (GenBank accession no. GQ329854), and the complete *ac* transcription unit. Images were collected using an Olympus BX-51 bright field microscope and processed with ImageJ and Adobe Photoshop. The homozygous deficiency line *Df(1) y ac* was used as a negative control, as this line carries a deletion of the genomic region encompassing the *y*, *yar*, and *ac* genes. Three biological replicates were performed.

Nuclear RNA isolation and analyses

Aged 6- to 12-hr embryos were collected on orange juice/agar plates, dechorionated with 50% hypochlorite solution, and frozen in liquid nitrogen. Frozen embryos were ground on dry ice, resuspended in buffer A (60 mM KCl, 15 mM NaCl, 15 mM Tris-HCl pH 7.4, 1 mM EDTA, 0.1 mM EGTA, 0.15 mM spermine, 0.45 mM spermidine, 0.45 mM DTT), and filtered through Miracloth (Calbiochem). The filtered material was split into two equivalent volumes ("total" and "nuclear"). The nuclear fraction was processed using nuclei isolation protocol as described previously (Parnell *et al.* 2003). RNA was isolated from both nuclear and total volumes using TRIzol extraction. Equal volumes were DNase I treated and reverse transcribed using High Capacity cDNA kit with random hexamer primers and analyzed by semi-quantitative PCR at 25 cycles for spliced transcripts and 30 cycles for intronic sequences. Amplified fragments were resolved on 1% agarose gel with ethidium bromide.

Northern analyses

Northern analyses were performed as described previously (Soshnev *et al.* 2008). Briefly, embryos were collected from *D. melanogaster* on orange juice and aged for 6–12 hr in a 25° incubator, while embryos were collected from *D. virilis* on grape juice plates and aged for 16–24 hr in a 20° incubator. RNA was isolated using TRIzol. Poly(A)$^+$ RNA was selected using Qiagen mRNA Midi kit, according to the manufacturer's instructions. Three to 10 μg of poly(A)$^+$ selected RNA were resolved on a formaldehyde–agarose gel, transferred to Nytran N membrane (Whatman), and hybridized to ^{32}P-dATP labeled DNA probes generated from *D. melanogaster yar* clone (GenBank accession no. GQ329854) or *D. virilis yar* cDNA. Membranes were exposed to X-ray film, stripped, and probed with a ^{32}P-dATP labeled DNA from the constitutively expressed *RpL32* gene as a loading control.

Enhancer-blocking assays

Insulator activity of the region encompassing the *yar* promoter was tested using two independent enhancer-blocking reporter *P*-element transposons. For these studies, a 150-bp fragment was PCR amplified from y^1 w^{67c23} genomic DNA, denoted *yarP*. This fragment includes MEME motif 1.1 (Figure 1) and contains two of the three *yar* transcription start sites. *yarP* was cloned between direct repeats of *loxP* sites and inserted either between the wing and body enhancers and promoter of the *y* gene to generate *P[yarP-yellow enhancer blocking (YEB)]* or between the eye enhancer and promoter of the *white* (*w*) gene to generate *P[yarP-white enhancer blocking (WEB)]* (Figure S3). For the *y* reporter, *yarP* was cloned in both orientations relative to the *y* promoter. As no differences in phenotypes were observed between transgenic lines carrying these distinct transposons, we represent these independent transposons together. *P*-element vectors were injected into the host y^1 w^{67c23} strain, and resulting progeny were screened for phenotypic changes indicative of carrying a second marker gene included on the transposon (Genetic Services, Cambridge, MA). Transgenic lines with single transposon insertions were established and analyzed. Phenotypes were determined by crossing transgenic males to y^1 w^{67c23} virgin females. Pigmentation of the wing and body cuticle in the resulting *P[yarP-YEB]* flies was determined in 3- to 4-day-old females, using a scale of 1–5, where 1 represents the null phenotype and 5 represents the wild-type state. Eye pigmentation in *P[yarP-WEB]* flies was determined in 3-day-old males and females, using a score of 1–5, where 1 represents white eyes and 5 represents red eyes. At least three independent crosses were set up for each genotype, and two people scored at least 20 flies from each cross. Lines that had low yellow pigmentation scores were analyzed further. In these cases, crosses were made with flies expressing Cre recombinase to catalyze excision of the *yarP*, as described previously (Chen *et al.* 2002). Resulting progeny were used to establish stocks. Confirmation of the deletion of the *yarP* was achieved by PCR analysis.

Ends-out gene targeting

Two transposons were constructed from the *pW25* targeting vector (Gong and Golic 2003, 2004), kindly provided by Kent Golic. *pW25* contains a multicloning site on either side of the w^{hs} gene flanked by *loxP* sites. The *P[ΔHR2 target]* (XGL440) transposon was generated to establish a 0.5-kb deletion encompassing *yarP*, which includes all three *yar* transcription start sites (Soshnev *et al.* 2008), whereas the *P[ΔHR1 target]* (MDW47) transposon was generated to establish a 0.2-kb deletion, which included *yarP* and twox of the three *yar* start sites. Both transposons were made in a two-step procedure. First, PCR primers containing *Not*I sites were used to isolate a 3.3-kb fragment (+6031 to +9318, relative to the *y* TSS, Δ*HR1*) or a 3-kb fragment [+6334 to +9318 relative to the *y* TSS, Δ*HR2*] of the

y–ac intergenic region. These PCR fragments were sequenced to confirm appropriate amplification. Second, the PCR fragments were cloned into XGL235, a derivative of *pW25* that carries a 6.6-kb *y* fragment (−1842 to +4796 relative to the *y* TSS), which includes the *y* transcription unit and the body enhancer, but lacks the wing enhancer, ultimately generating the targeting transposons. Transgenic lines of *P[ΔHR1 target]* and *P[ΔHR2 target]* were established by transformation of y^1 w^{67c23} flies. Gene targeting was completed followed the procedure outlined in Gong and Golic (2004), screening for flies with darkly pigmented wings, to generate $yar^{\Delta HR1w}$ and $yar^{\Delta HR2w}$. Next, the w^{hs} gene was removed by crossing red-eyed males carrying the targeted *yar* deletion to females carrying Cre recombinase, as described in Chen *et al.* (2002). The white-eyed flies were collected and used to establish homozygous stocks, called $yar^{\Delta HR1}$ and $yar^{\Delta HR2}$. A combination of Southern and PCR analyses identified correctly targeted events (Figure S4).

Real-time PCR analyses

RNA was isolated from embryos from three lines: Canton S, $yar^{\Delta HR1}$ line MDW47 43-1, and $yar^{\Delta HR2}$ line XGL440-114. RNA isolation and quantitative real-time PCR analyses were performed (Parnell *et al.* 2006). Primer sequences are shown in Table S1. Values obtained from technical replicates for each PCR amplification were averaged, with no greater than 0.5 cycle threshold (Ct) seen between replicates. Two to three experiments were performed for each primer set from at least two independent RNA samples. The expression level of each gene was determined using *RpL32* as an internal control (ΔCt). The fold change in expression of each gene relative to the wild-type (Canton S) value was determined with the ΔΔCT method.

Reactive climbing assays

Climbing assays were performed as described previously (Pinto *et al.* 2008). Five males and five females for each genotype were collected 1 day after eclosion and housed in individual vials at 25°, 70% humidity, with a 12 hr day/night cycle. Five-day-old flies were placed in a 15-cm-long by 1.5-cm-wide graduated glass cylinder. The flies were equilibrated for several minutes, tapped to the bottom, and allowed to climb up the sides. The number of flies that crossed the 15-cm mark in a 30-sec time was recorded. This procedure was repeated five times with five replicates for each genotype (n = 25). The average of these replicates was plotted as the percentage of flies that climb 15 cm in 30 sec. The $dMAN1^{\Delta 81}$ null mutant was used as a positive control (Pinto *et al.* 2008).

Sleep pattern analyses and yar rescue

Three- to 5-day-old virgin females were individually housed in a glass tube (5 [W] × 65 [L] mm) with regular fly food and subjected to 12-hr light and 12-hr dark cycles at 25°. Flies were acclimated to the experimental conditions for 1 day and then their locomotor activity was monitored using the *Drosophila* Activity Monitor system (Trikinetics). Locomotor activity data were collected at 1-min intervals for 3 days and analyzed with a Microsoft Excel-based script as described previously (Hendricks *et al.* 2003; Kume *et al.* 2005). Sleep was defined as ≥5 min of behavioral immobility in the DAM system.

To establish a genomic *yar* rescue construct *P[yar w]*, a 6-kb *yar* genomic region was amplified (+4674 to +10696 relative to the *y* TSS), sequenced and cloned into the CaSpeR3 *P*-element vector carrying *mini-w* selectable marker (Figure 3). The rescue construct was injected directly into the $yar^{\Delta HR2}$ background produced by homologous recombination (Genetic Services). Transgene insertions were identified by phenotypic rescue of the mutant eye color. Homozygous stocks were established by crossing $yar^{\Delta HR2}$, *P[yar]* males and virgin females together to obtain homozygous *P[yar]* insertions in the same genetic background as the *yar* mutants. Southern analyses determined the structure and number of transgenes. Flies from two independent transformed lines were analyzed.

Results

Conservation of yar

The *yar* gene is located ∼1.2 kb downstream of *y* and ∼3.0 kb upstream of *ac* (Figure 1). To address whether *yar* is conserved, we compared genomic sequences of the *y–ac* intergenic region from *D. melanogaster* with eight *Drosophila* species. In these analyses, we included the region upstream of *ac* for *D. mojavensis*, the exceptional *Drosophila* species that does not have *y* linked to *yar* (Negre and Simpson 2009). Intergenic regions were analyzed using MultiPipMaker, a program that constructs multisequence alignments on the basis of percentage of identity plots (PIPs) from pairwise comparisons (Schwartz *et al.* 2000) and MEME, a sequence analysis program that identifies statistically supported conserved motifs, on the basis of length, similarity, and number of occurrences within and among the sequence set (Bailey *et al.* 2006). These analyses revealed multiple aligned regions that decreased in size with increasing evolutionary distance (Figure 1A). We identified eight motifs of identical order and orientation present in all species, with the exception of *D. grimshawi*, where fewer motifs were found due to a gap in the available genome sequence (Figure 1, Figure S1, Table S2). The sizes of the conserved motifs ranged from 40 (motif 2.4) to 111 bp (motif 2.1), showing extensive sequence identity. Motifs of conservation largely localize within or near the *yar* transcription unit. While four of the identified MEME motifs correspond to *yar* exons, none encompassed the short open reading frames of the potential polypeptides, providing further evidence that *yar* encodes lncRNAs. These findings extend previous analyses comparing *D. melanogaster* and *D. virilis* sequences that identified motifs 1.1 and 1.4, which lie upstream of the dorsocentral enhancer (Garcia-Garcia *et al.* 1999).

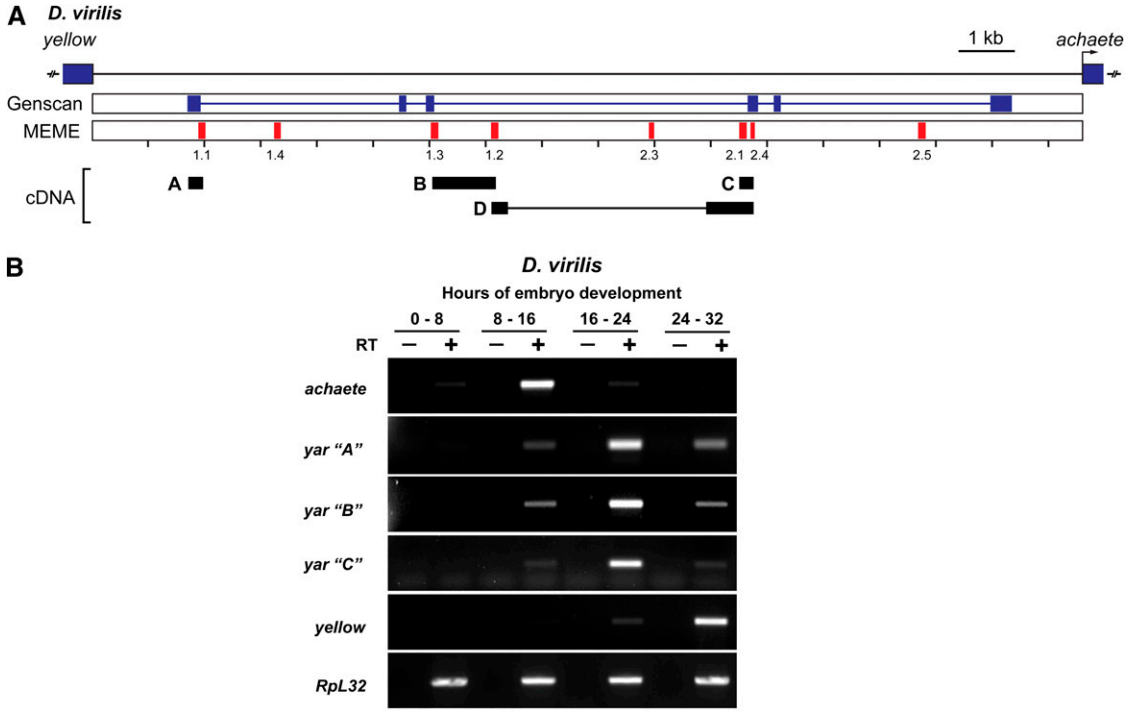

Figure 2 *yar* is conserved in *D. virilis*. (A) Structure of the *D. virilis* 17-kb *y–ac* intergenic region. The positions of the *y* and *ac* genes are shown by rectangles. The Genscan-predicted gene (blue) and MEME-identified motifs (red) are indicated below. Four cDNAs (A–D) obtained from PCR analyses are shown; the thin line in cDNA D indicates an intron. (B) Semiquantitative PCR analyses of RNAs isolated during the indicated times of *D. virilis* embryogenesis. Primer pairs corresponding to *ac*, three of the *yar* cDNAs, and *y* were analyzed. *RpL32* represents a constitutively expressed RNA and serves as a control. The (−) RT lanes control for genomic DNA contamination. RNAs were isolated from aged embryos, as indicated by hours of development.

We noted that one of the largest most conserved motifs in the *y–yar–ac* region corresponded to motif 1.1, implying that transcription of *yar* might be conserved. To test this postulate, we determined whether *yar* was expressed in *D. virilis*, a species separated from *D. melanogaster* by 40–60 MY of evolution. RNA was isolated from *D. virilis* embryos, a developmental stage of maximal expression of *D. melanogaster yar* (Chia *et al.* 1986; Soshnev *et al.* 2008). Northern analysis of poly(A)$^+$ RNA identified a major *D. virilis* transcript of ~2.5 kb that accumulates in midembryogenesis, although at much lower levels than the major *D. melanogaster yar* transcript (Figure S2A). Semiquantitative reverse transcriptase polymerase chain reaction (RT-PCR) studies were undertaken to define the expression pattern for *D. virilis* RNAs generated in the *y–ac* intergenic region. Using primer pairs anchored in the conserved MEME motifs, the expression of four cDNAs was studied during three stages of embryonic development (Figure 2, Figure S2B). Importantly, the expression pattern of these cDNAs was coordinated. The temporal accumulation of *yar* in *D. virilis* embryos was reminiscent of *D. melanogaster*, with transcription of *yar* coinciding with *ac* down-regulation and transcription of *y* coinciding with *yar* down-regulation. Sequence analysis of these *D. virilis* cDNAs showed that the coding capacity of each was <75 amino acids, with no evidence of sequence conservation with the potential *D. melanogaster* polypeptides (data not shown). A novel *D. virilis* gene was predicted within the *y–ac* intergenic region using Genscan (Burge and Karlin 1997) (Figure S2A). The exons of the Genscan-predicted gene were close to the identified MEME motifs, with three motifs showing a partial overlap with the predicted Genscan exons. We completed RT-PCR analyses to

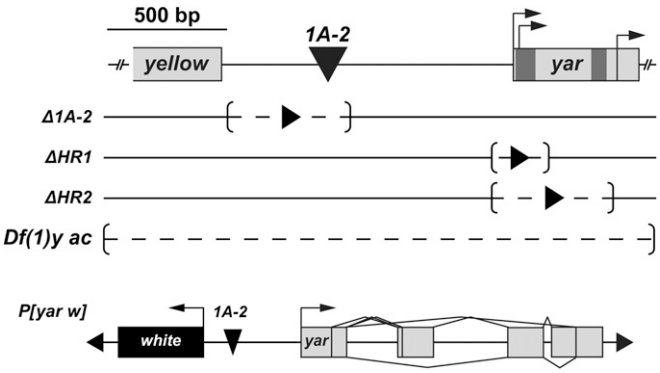

Figure 3 Structure of the *yar* alleles used in the study. (Top) Schematic of the genomic region encompassing the 3′ end of *y*, the 1A-2 element (inverted triangle), and the first exon of *yar*. Previously identified alternative start sites are indicated by bent arrows (Soshnev *et al.* 2008). Motifs 1.1 and 1.4 are colored by darker shading in the *yar* gene. (Middle) Structure of the *yar* deletion alleles obtained by homologous recombination. Dashed line in brackets indicates deleted region; solid arrowhead represents the residual *loxP* site. The extant allele *Df(1) y ac* removes the region spanning the whole *y–yar–ac* locus. (Bottom) Structure of the *P[yar w]* transgene used in the rescue studies.

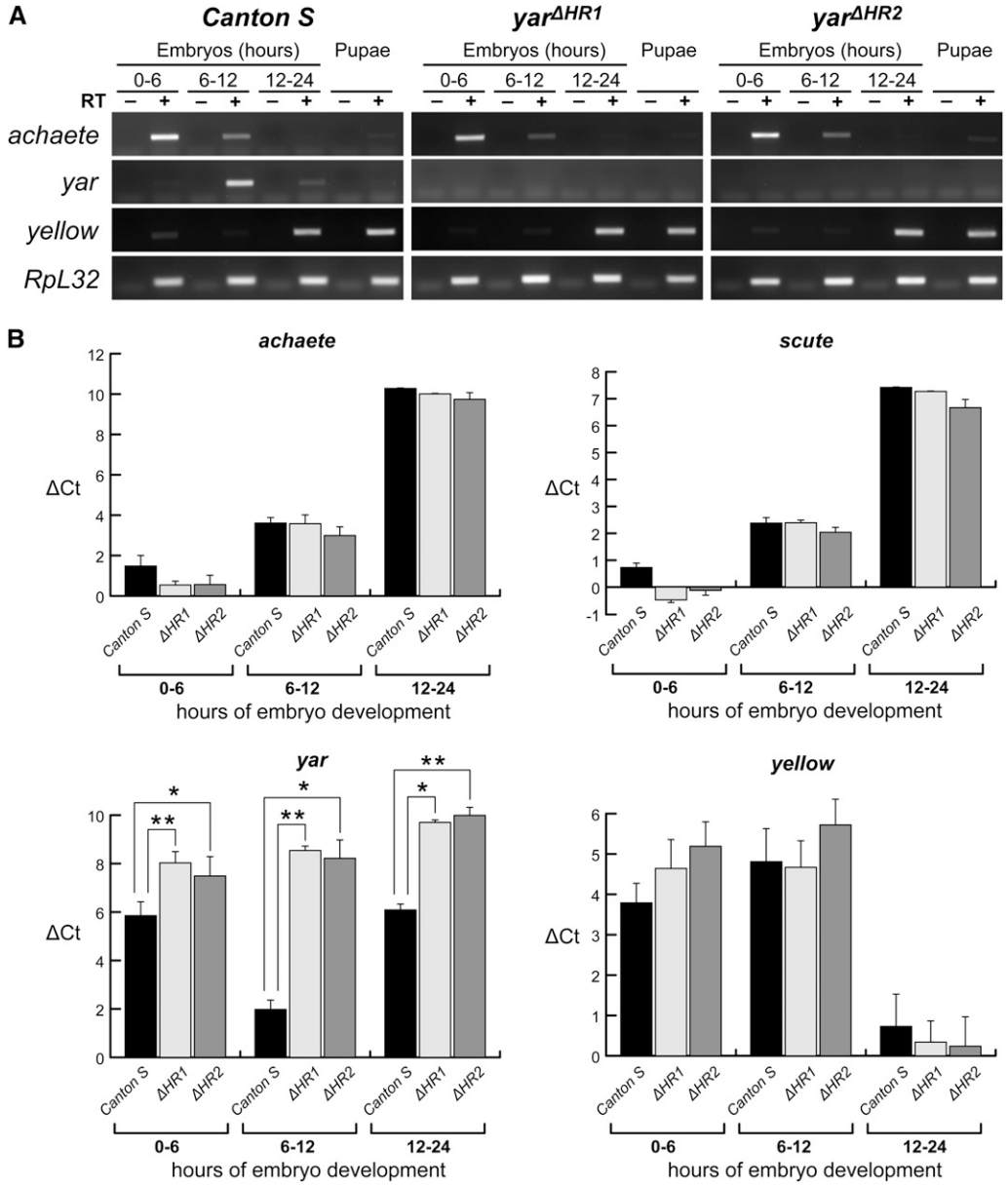

Figure 4 Quantitative analyses of gene expression in *yar* null mutants. RNA was isolated from wild type (Canton S) and the *yar* null mutants [$yar^{\Delta HR1}$ (Δ*HR1*) and $yar^{\Delta HR2}$ (Δ*HR2*)]. (A) Semiquantitative PCR analyses of RNAs isolated from aged embryos and mixed stage pupae. *RpL32* is a constitutively expressed gene and serves as a loading control. The (−) RT lanes control for genomic DNA contamination. (B) Quantitative RT-PCR of *y*, *yar*, *ac*, and *sc*, the gene downstream of *ac*. Cycle threshold (Ct) values were normalized to the constitutively expressed *Ras64B* gene to control for the amount of input cDNA (ΔCt). A higher ΔCt value indicates lower level of RNA accumulation. Error bars indicate standard deviation from two biological replicates. Asterisks indicate statistical significance by Student's *t*-test, $*P < 0.05$, $**P < 0.01$.

test the accuracy of the Genscan representation (Figure S2B). Primer pairs anchored within the predicted exons failed to amplify *D. virilis* embryonic cDNAs. Further, tests using mixed primer pairs, including between one MEME motif primer and one Genscan exon primer, were only successful in one case (product A, Figure S2B). On the basis of these findings, we conclude that the Genscan prediction does not accurately reflect the *D. virilis y–ac* intergenic transcription unit. Taken together, our data provide compelling support that *yar* is a conserved lncRNA gene.

Several experiments tested the function of the conserved MEME motifs. First, we tested whether motif 1.1 had insulator activity. These experiments were predicated on previous studies showing that in certain genetic contexts, the enhancers of the *y* and *ac* genes were capable of directing inappropriate transcription (Campuzano *et al.* 1986; Parnell *et al.* 2003). Such observations imply that independent transcriptional regulation of the *y* and *ac* genes requires the presence of an intervening chromatin insulator. Many insulators have been associated with promoter activity (Kuhn and Geyer 2003; Chopra *et al.* 2009; Raab and Kamakaka 2010), consistent with the location of two out of three *yar* promoters within motif 1.1 (Soshnev *et al.* 2008). To this end, we tested the enhancer blocking capacity of motif 1.1 using two well-characterized reporter genes (Figure S3). Analysis of transgenic flies carrying these reporter genes showed that enhancer blocking did not occur, implying that motif 1.1 is not an insulator. Second, we investigated whether the conserved motifs, or other regions within the *yar* transcription unit, were processed into smaller RNAs, such as miRNAs. In these analyses, existing miRNA databases (Kozomara and Griffiths-Jones 2011), as well as

structural predictions using Mfold were employed (Zuker 2003). These strategies provided no evidence for the generation of miRNAs from *yar* (data not shown).

Distribution of yar during embryogenesis

To gain insights into the function of *yar*, we examined the spatial distribution of this RNA during embryogenesis (Figure 1B). Whole mount *in situ* RNA hybridization was performed in aged embryos using probes corresponding to *yar*, *y*, and *ac*. The *y* and *ac* probes served as positive controls because the accumulation of these RNAs was previously defined (Romani *et al.* 1987; Walter *et al.* 1991). As a negative control, *Df (1) y ac* embryos were studied in parallel. These embryos carry a deletion of all three genes, thereby providing a null background. As expected, accumulation of *ac* RNA was restricted to neurogenic regions, while accumulation of *y* RNA was limited to stripes that underlie the ventral denticle belts. In contrast, *yar* RNA was found throughout the embryo (Figure 1B). In all cases, the level of hybridization for each probe was higher in wild-type embryos than in the *Df(1) y ac* controls. These data indicate that *yar* is globally expressed during embryogenesis.

The function of lncRNAs depends upon their subcellular location. As lncRNAs can localize to the nucleus and cytoplasm, we determined which subcellular compartment contains *yar*. In these experiments, RNA was isolated from unfractioned or nuclear fractions of homogenates made from 6- to 12-hr wild-type embryos (Figure 1C). These RNA samples were reverse transcribed and the level of *yar* was determined by PCR. *Ras64B* was chosen as a control because this gene encodes a globally expressed, spliced protein-coding mRNA. The PCR analyses involved two sets of primer pairs for analysis of *yar* and *Ras64B* RNAs (Table S1). For one pair, opposing primers were positioned at opposite exon junctions spanning a common intron to detect mature RNA. For the second pair, opposing primers were located within intronic sequences, which are expected to be nuclear restricted. We obtained a PCR product representing the mature *yar* RNA only from the sample of total RNA, whereas a PCR product representing *yar* intronic sequences was detected in both nuclear and total RNA (Figure 1C). These data imply that spliced *yar* RNAs are cytoplasmic, a conclusion that is supported by analyses of *Ras64B* RNA.

Investigation of yar contributions to the regulation of neighboring gene expression

Recent studies demonstrate that lncRNA genes regulate transcription both in *cis* and *trans* (Ogawa and Lee 2002; Martens *et al.* 2004; Petruk *et al.* 2006; Martianov *et al.* 2007; Barrandon *et al.* 2008; Brock *et al.* 2009; Mercer *et al.* 2009; Taft *et al.* 2010). The genomic location of *yar*, coupled with the conserved timing of embryonic expression, suggested that *yar* might regulate transcription of the adjacent *y* or *ac* genes. This postulate is supported by examples where transcription of an upstream noncoding RNA gene represses expression of the adjacent downstream gene by transcriptional interference (Martens *et al.* 2004; Petruk *et al.* 2006). Two observations supported that repression of *ac* would require *yar* transcription, and not *yar* RNA production. First, *yar* is a cytoplasmic RNA (Figure 1C), unlike nuclear lncRNAs that have a direct role in gene silencing. Second, the timing and level of *ac* and *y* expression are unchanged when levels of *yar* are reduced, as defined in studies of the hypomorphic $yar^{\Delta 1A\text{-}2}$ mutant (Soshnev *et al.* 2008).

We generated two null alleles using ends-out gene targeting to test the role of *yar* transcription on neighboring gene expression. These experiments deleted either 200 bp ($yar^{\Delta HR1}$) or 500 bp ($yar^{\Delta HR2}$) of the *yar* promoter, removing two or three of the *yar* transcription start sites (Figure 3, Figure S4), respectively. Quantitative real-time PCR analyses demonstrated that $yar^{\Delta HR1}$ and $yar^{\Delta HR2}$ flies had 85-fold lower levels of *yar* RNA relative to Canton S, which were undetectable in agarose gel analyses (Figure 4). Measured levels of *yar* RNA in $yar^{\Delta HR1}$ and $yar^{\Delta HR2}$ flies was similar to those obtained from flies carrying a deletion of the *yar* locus (*Df (1) y ac*, data not shown), consistent with our prediction that the newly generated alleles remove the *yar* promoter. Using $yar^{\Delta HR1}$ and $yar^{\Delta HR2}$ mutants, we defined the timing and level of *y*, *ac*, and *scute* (*sc*) RNA using quantitative real-time PCR analyses. We found that embryonic expression of all genes was unchanged by loss of *yar* transcription (Figure 4). We conclude that *yar* does not contribute to the regulation of transcription of neighboring genes.

Functional analysis of yar

Visual inspection of *yar* mutant flies revealed no overt morphological defects. The absence of changes in bristle number and cuticle pigmentation is consistent with normal transcription of the neighboring *y* and *ac* genes (Figure 4). A possible functional role for *yar* was suggested by consideration of the functions of the neighboring *y*, *ac* and *sc* genes. The *ac* and *sc* genes encode basic helix–loop–helix transcription factors required for formation of neural precursors (Modolell and Campuzano 1998), while the *y* gene encodes a secreted protein required for male sexual behavior (Nash and Yarkin 1974; Biessmann 1985; Chia *et al.* 1986; Geyer *et al.* 1986; Drapeau *et al.* 2003, 2006). These observations suggested that *yar* resides in a cluster of neural genes. As emerging evidence suggests that gene order within eukaryotic chromosomes is nonrandom (Lee and Sonnhammer 2003; Hurst *et al.* 2004; Yi *et al.* 2007; de Wit and van Steensel 2009), we predicted that *yar* may have a neural function.

One of the ultimate manifestations of neural function is behavior. To address possible roles of *yar* in fly behavior, two assays were used. First, we evaluated the general locomotor and geotactic ability in *yar* mutants. Second, we examined sleep, a fundamental biological process conserved among evolutionarily diverse animal species (Sehgal *et al.* 2007; Cirelli and Bushey 2008; Cirelli 2009). In both sets of experiments, flies corresponding to multiple independently generated *yar* mutant alleles were tested. We used homozygous

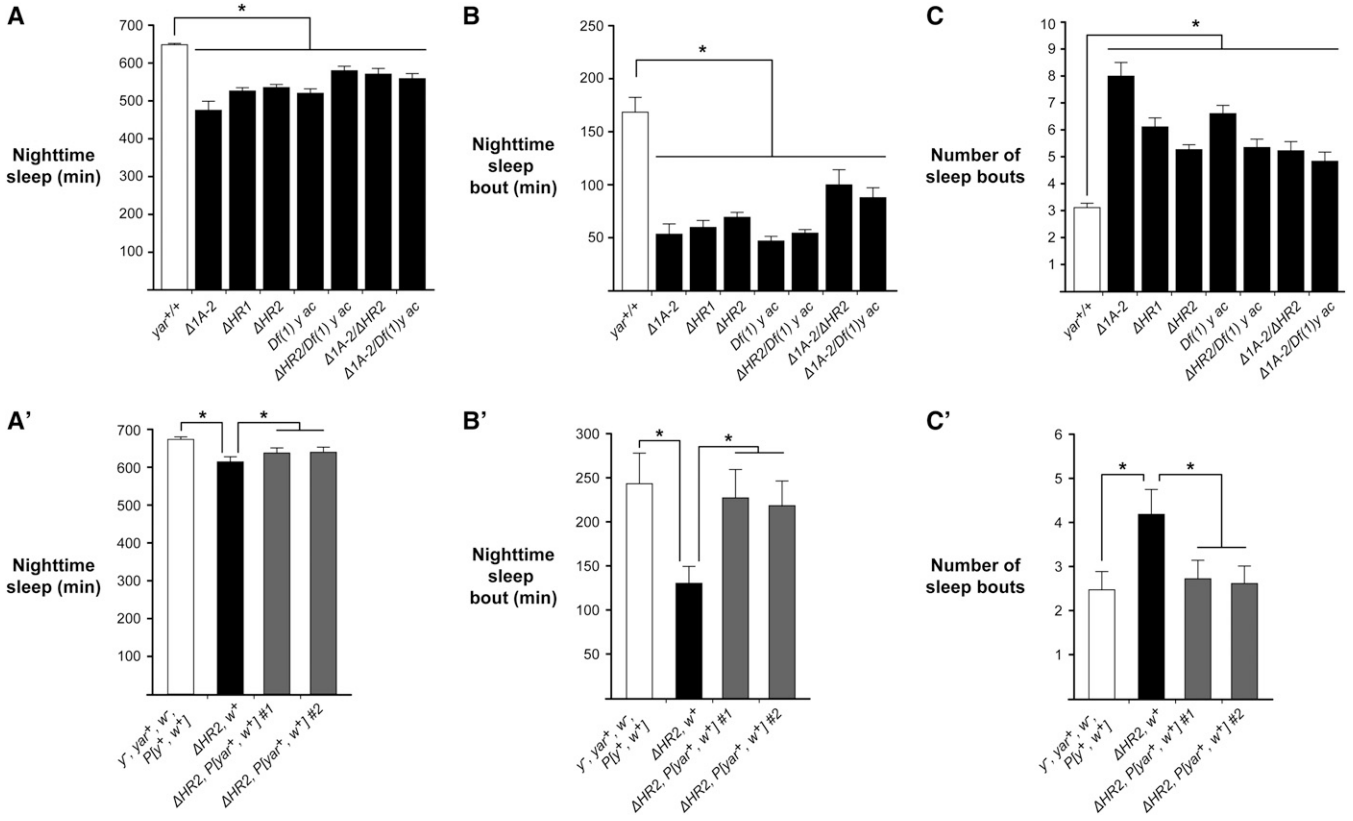

Figure 5 Loss of *yar* affects sleep behavior in *Drosophila*. (A) Baseline nighttime sleep in the parental $yar^{+/+}$ (y^1 yar^+ w^{67c23}, open bar) line and *yar* mutants (y^1 yar^{mutant} w^{67c23}, solid bars). Average amounts of sleep for 3- to 5-day-old virgin females are shown ($n \geq 32$). (B and C) Average duration of nighttime sleep bout and number of sleep episodes. (A′) Effect of rescue by *P[yar w]* on nighttime sleep duration. Shown are data obtained from the parental line (y^1 yar^+ w^{67c23}, *P[ΔHR2 target]*, open bar), the *yar* mutant (Δ*HR2*, solid bar). and the *yar* mutant carrying the *P[yar w]* rescue construct inserted at two independent genomic locations (Δ*HR2 R1* and Δ*HR2 R2*, shaded bars). (B′ and C′) Effects of the rescue *P[yar w]* transposon on sleep bout duration and number of sleep bouts in *yar* mutants. Kruskal–Wallis one-way ANOVA, $*P < 0.05$. Error bars represent SEM.

and heteroallelic mutant combinations to assay behavior in multiple distinct genetic backgrounds. We tested four *yar* alleles, including one hypomorphic ($yar^{\Delta 1A\text{-}2}$) and three null ($yar^{\Delta HR1}$, $yar^{\Delta HR2}$, and *Df(1) y ac*) alleles (Figure 3). We reasoned that if consistent behavioral changes were observed, then these data would support a neural function for *yar*.

In reactive climbing assays, three groups of 10 flies for each *yar* genotype were analyzed. These flies were placed in a graduated cylinder, tapped to the bottom, and the number of flies climbing to 15 cm in 30 sec was recorded. These studies showed that flies with decreased or eliminated *yar* RNA had normal climbing activity (data not shown). These experiments suggest that general locomotion and the tendency of flies to move against gravity are not perturbed.

The *Drosophila* Activity Monitoring (DAM) system was used to evaluate sleep behavior in *yar* mutants. In these studies, individual flies were loaded into an activity monitor tube and a computer recorded each time a fly crossed an infrared beam that bisects the tube. Previous studies have defined sleep as a period of quiescence lasting ≥5 min (Hendricks *et al.* 2000; Shaw *et al.* 2000). Parameters of sleep depend upon sex and age of the fly (Cirelli 2006, 2009; Koh *et al.* 2006; Sehgal *et al.* 2007). Here, we studied sleep behavior in 3- to 5-day-old females. We tested females carrying different homozygous and heterozygous combinations of *yar* alleles representing different genetic backgrounds. Each of these *yar* mutant backgrounds carried a deletion of the *w* gene (the w^{67c23} allele), a mutation that has significance to behavior assays. The *w* gene encodes an adenosine triphosphate (ATP)-binding cassette (ABC) transmembrane transporter protein (Mount 1987; Pepling and Mount 1990; Anaka *et al.* 2008), and affects fly behavior (Zhang and Odenwald 1995; Cirelli *et al.* 2005; Anaka *et al.* 2008). For this reason, our reference line carried a wild-type *yar* gene and the *w* deletion allele.

Females of each genotype were placed in activity monitor tubes and acclimated for 1 day. Locomotor activity was assessed at 1-min intervals over a 3-day period of consecutive 12-hr light (day) and dark (night) cycles. From these data, we determined the average time spent in nighttime sleep. We found that all *yar* mutant females showed a significant decrease in the level of total nighttime sleep, irrespective of mutant genotype (Figure 5A). Even though nighttime sleep in *yar* mutants was reduced, sleep remained higher in the night than day, indicating sleep reduction occurred in the context of a normal circadian rhythm. Further,

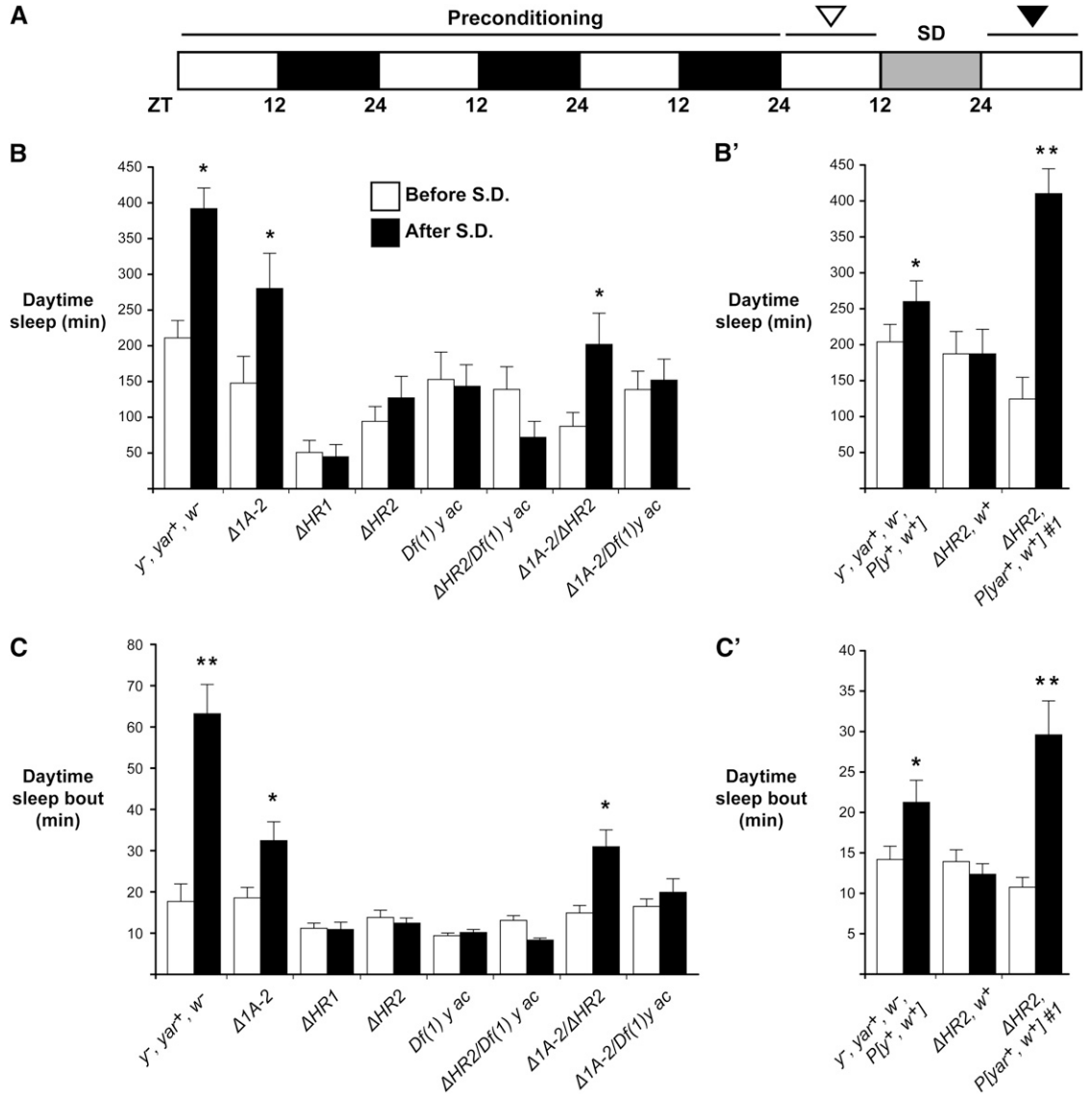

Figure 6 Loss of *yar* causes defect in homeostatic regulation of sleep. (A) Diagram of experimental strategy for determining effects of sleep deprivation. Flies were preconditioned in the DAM system for 3 days of 12-hr day and night cycles, and baseline daytime sleep bout duration was established on day 4 (open arrowhead). Flies were sleep deprived for one night (SD) and sleep parameters were measured the following morning (solid arrowhead). (B) Total daytime sleep before (open bars) and after (solid bars) sleep deprivation is shown. (C) The average length of sleep bouts before and after sleep deprivation. (B′ and C′) Response to sleep deprivation in the w^+ reference and yar mutants carrying the *P[yar w]* rescue transgene. Kruskal–Wallis one-way ANOVA, $*P < 0.05$, $**P < 0.001$. Error bars represent SEM.

yar mutants retained a circadian rhythm even when placed in total darkness for 10 days (Figure S5A). We assessed whether decreased sleep resulted from increased activity during nighttime periods of wakefulness. To this end, we divided the total activity counts by the total length of waking time. These calculations showed that the nighttime activity of *yar* mutants was not elevated compared to the reference strain (Figure S5B), indicating that reduced sleep is not due to a general increase in locomotion activity. To characterize the architecture of nighttime sleep, we analyzed the duration and number of sleep bouts in *yar* mutants relative to the reference strain. Notably, we observed that the length of nighttime sleep bouts was shortened in *yar* females, coinciding with an increase in the number of sleep episodes (Figure 5, B and C). These data indicate that *yar* mutants have reduced and fragmented sleep patterns. Similar findings were observed for males (data not shown).

A complementation assay was used to determine whether the altered sleep behaviors were caused by a loss of *yar*. In these studies, $yar^{\Delta HR2}$ w^{67c23} flies were directly transformed with a *P[yar w]* transposon, to ensure that the mutant and *P[yar w]* transgenic flies had isogenic backgrounds. The *P[yar w]* transposon contains a genomic fragment encompassing the *yar* transcription unit, with ~1.2 kb of upstream and ~0.15 kb of downstream flanking DNA linked to the *mini-w* reporter gene (Figure 3). To assess effects of

reintroduction of *yar*, we changed our reference line to reflect that the *P[yar w]* transposon carries a mini-*w* gene. The reference line, called yar^{+} w^{+}, carried the w^{67c23} mutation and a *P* transposon with the mini-*w* transgene. We measured sleep parameters in females from two independent $yar^{\Delta HR2}$, *P[yar w]* transgenic lines, in which the rescue transposon was located at a different genomic locations [rescue 1 (R1) and rescue 2 (R2)]. We found that reintroduction of the *yar* genomic fragment restored the total amount of nighttime sleep (Figure 5A′). Significantly, sleep bout length was increased in both independent $yar^{\Delta HR2}$, *P[yar w]* lines, while the number of sleep episodes was decreased (Figure 5, B′ and C′). These data indicate that reintroducing *yar* restored sleep parameters, providing strong evidence that *yar* plays a role in sleep regulation.

Sleep has a homeostatic component, in which individuals regain lost sleep after deprivation (Ho and Sehgal 2005; Cirelli 2009). We tested whether loss of *yar* affected homeostasis. In these studies, reference females and females corresponding to multiple *yar* genotypes were placed in activity monitor tubes, preconditioned for 3 days of 12-hr light and dark cycles, followed by 12 hr of mechanical sleep deprivation during the fourth night (Figure 6A). The amount of daytime sleep was assessed prior to (third and fourth days) and after (fifth day) sleep disruption. We found that daytime sleep bout length did not change between days 3 and 4 for either the reference or *yar* mutant females (data not shown), indicating that time spent in the activity tubes did not influence sleep. However, following sleep deprivation, reference females increased total daytime sleep and sleep bout length. In contrast, no increase in these parameters was observed for *yar* mutants, with one exception (Figure 6, B and C). The exceptional females were $yar^{\Delta 1A\text{-}2}$, where daytime sleep was increased, but to a lower level than the reference line. The ability of $yar^{\Delta 1A\text{-}2}$ females to respond to sleep deprivation may reflect the presence of low levels of *yar* RNA (Soshnev *et al.* 2008), a proposal supported by findings that sleep rebound was lowered or lost in females that were heterozygous for $yar^{\Delta 1A\text{-}2}$ and a *yar* null allele (Figure 6, B and C). Importantly, defects in sleep homeostasis were rescued by introduction of *P[yar w]*. The rescued $yar^{\Delta HR2}$, *P[yar w]* females showed increased daytime sleep due to lengthened sleep bouts following sleep deprivation compared to the isogenic $yar^{\Delta HR2}$ females (Figure 6, B′ and C′). Together, these data suggest that *yar* mutants display an altered homeostatic sleep response.

Discussion

yar is a conserved lncRNA gene

The *yar* gene resides within a cluster of neural genes, separating the well-characterized *y* and *ac* genes. The architecture of this region has been cited as a paradigmatic example of gene organization and function, because the order and orientation of these genes remains unchanged within genomes of distantly related insect species (Garcia-Bellido and De Celis 2009; Negre and Simpson 2009). However, these previous analyses did not recognize the presence of *yar*, likely because *yar* generates transcripts that lack a large ORF (Soshnev *et al.* 2008). In our studies, we obtained several lines of evidence demonstrating that *yar* is conserved within *Drosophila* species. First, genomic comparisons of the *y–ac* intergenic region identified eight conserved motifs that largely map to the *yar* transcription unit (Figure 1). Second, one of the most highly conserved motifs, motif 1.1, encompasses the *yar* promoters and regulates *yar* transcription. Importantly, motif 1.1 is not a regulatory element for either *y* or *ac*, as deletion of this region eliminates *yar* expression, without affecting transcription of neighboring genes (Figure 4). Third, the temporal pattern of embryonic transcription of *yar* is conserved in *D. virilis (*Figure 2). These data suggest that *yar* is conserved in drosophilids.

The *yar* gene was classified as an lncRNA gene on the basis of the absence of an ORF >75 amino acids. While the requirement for a large ORF is commonly used to distinguish ncRNAs, emerging evidence suggests that caution is needed when this is the only parameter used for lncRNA designation (Galindo *et al.* 2007; Kondo *et al.* 2007; Hanyu-Nakamura *et al.* 2008; Hashimoto *et al.* 2008; Timinszky *et al.* 2008). For example, the *tarsal-less/polished rice* (*tal/pri*) gene was originally identified as a putative mRNA-like lncRNA (Inagaki *et al.* 2005; Tupy *et al.* 2005). Subsequent analyses showed that *tal/pri* transcripts encode short peptides of 11 amino acids that contain full biological function (Galindo *et al.* 2007; Kondo *et al.* 2007). In cases where small peptides have been identified, evolutionary comparisons have demonstrated conservation of the small ORFs. To this end, we examined whether the eight conserved motifs provide evidence for a conserved coding capacity in *yar* transcripts. Of the eight, four motifs reside within *yar* exons but do not overlap with the putative short ORFs (Figure 1, Figure S1). Of the four motifs located within *yar* exons, only motif 1.3 contains an ATG; translation at this codon would generate a peptide of three amino acids. Further, our analysis of *D. virilis yar* transcripts failed to identify conservation with any of the potential *D. melanogaster* polypeptides. Together, these findings provide strong evidence that *yar* is a lncRNA gene.

yar is a cytoplasmic RNA

LncRNAs have been identified that localize to specific subcellular compartments. A large and growing list of lncRNAs are retained in the nucleus, where they contribute to nuclear organization and gene expression (Mercer *et al.* 2009; Chen and Carmichael 2010; Taft *et al.* 2010; Clark and Mattick 2011). A smaller number of lncRNAs have been characterized that function in the cytoplasm, with *yar* falling into this second class (Panzitt *et al.* 2007; Matouk *et al.* 2009; Wang *et al.* 2010; Clark and Mattick 2011). One of these cytoplasmic lncRNAs is the **h**ighly **u**p-regulated in **l**iver **c**ancer (HULC) RNA, discovered in expression array studies that identified genes misregulated in hepatocellular

carcinoma (Panzitt *et al.* 2007). Functional analyses of HULC found that this lncRNA contributes to a regulatory circuit that modulates miRNA activities, acting as a sponge to down-regulate a series of miRNAs (Wang *et al.* 2010). Similarly, RNAs generated from pseudogenes have been found to act as decoys for miRNAs by modulating interactions between miRNAs and target coding mRNAs (Poliseno *et al.* 2010). Prompted by these observations, we investigated a possible link between *yar* and *Drosophila* miRNAs. To this end, sequences encompassing the *yar* exons (2 kb) were submitted to the Web-based tool MicroInspector (Rusinov *et al.* 2005). We identified the presence of miRNA seed matches with a high free energy cutoff value of −25 kcal/mol at the temperature of 25°, using the Release 17 of Sanger Institute miRBase that includes both computationally predicted and experimentally confirmed miRs. These analyses uncovered 33 miRNA seed matches within *yar* exons corresponding to 19 confirmed miRNAs (Figure S6, Table S3). Of the exonic seeds for miRNAs, six map within the conserved motifs 1.1, 1.2, and 1.4, with one miRNA (dme-miR-4970-5p) having three seed matches within the *yar* exons. These data support a possible connection between *yar* and miRNA regulation. As a control, we submitted sequences corresponding to the *yar* intron (2.8 kb). These analyses identified 36 miRNA seed matches that correspond to 25 confirmed miRNAs (Figure S6, Table S3). Of the confirmed intronic miRNAs, one has two seed matches. These observations indicate that the *yar* exons are not enriched for miRNA sequences relative to control, a finding consistent with the small size of the miRNA seeds. Further studies are necessary to discern the functional significance between *yar* and the miRNAs, experiments that require an understanding of the targets of the *yar* exonic miRNAs, which are largely unknown at this time. Even so, we note that *yar* and many *Drosophila* lncRNAs are expressed during early embryogenesis following the developmental period of active changes in mRNA stability. As recent studies suggest that miRNAs promote turnover of maternal and zygotic RNAs (Bushati *et al.* 2008; Thomsen *et al.* 2010), these observations raise the possibility that *yar* and other cytoplasmic lncRNAs may function as sponges that titrate miRNAs during embryogenesis, permitting fine-tuning of the miRNA-dependent degradation pathway.

Loss of yar disrupts sleep regulation

Phenotypic analyses of *yar* mutants demonstrate that *yar* is required for both sleep maintenance and homeostasis. We find that nighttime sleep is decreased in loss-of-function *yar* mutants, correlating with reduced sleep bout length. Further, sleep homeostasis is affected by *yar* loss, as these mutants do not increase daytime sleep following sleep deprivation. Both defects are restored by introduction of the *yar* gene, providing compelling evidence that *yar* is required for sleep regulation. The *yar* mutant phenotypes are reminiscent of those described for mutations in the serotonin receptor 1A gene (Yuan *et al.* 2006), which affects sleep due to defects in the adult mushroom bodies. It is unclear whether the requirement for *yar* is developmental or due to a physiological role in sleep regulation. While *yar* expression is highest during early embryogenesis, recent deep sequencing studies have uncovered *yar* RNAs in poly(A)$^+$ RNA isolated from male and female heads (Graveley *et al.* 2011). These data suggest that *yar* might directly regulate processes in the brain that impact sleep behavior. Of note, one of the miRNA seed matches within the *yar* exon corresponds to miRNAs from the miR-310 cluster (Figure S6), a match not found in similar analyses of *yar* intronic sequences or exonic sequences corresponding to three other genes (*y*, *ac*, and *GAPDH2*; data not shown). Loss of miRNAs 310 to 313 alters synaptic transmission at the larval neuromuscular junction, with no effect on viability or fertility (Tsurudome *et al.* 2010). These findings are consistent with the possibility that *yar* might participate in a regulatory circuit that influences levels of miRs within the brain, which may have the capacity to contribute to synaptic homeostasis. Further studies are needed to elucidate the temporal and tissue-specific requirements for *yar*, which will provide insights into how *yar* contributes to sleep regulation.

Many *Drosophila* lncRNA genes display spatially restricted embryonic expression that corresponds to RNA accumulation in the developing central and peripheral nervous system (Inagaki *et al.* 2005; Li *et al.* 2009). These observations suggest that ncRNAs might commonly contribute to neuronal function during *Drosophila* development. Further, large numbers of ncRNAs have been identified in mouse brain (Mercer *et al.* 2008), suggesting that such functions might extend to vertebrates.

Acknowledgments

We thank the members of Geyer and Kitamoto laboratories for critically reading this manuscript. We thank Kate Appleton, Kate Jandacek, Will Barry, and Yasir Ahmed for technical assistance. We thank Yikang Rong for providing *pW25* and Kent Golic for providing the *70FLP* and *70I-SceI* flies. This work was supported by National Institutes of Health Grant GM42539 to P.K.G.

Literature Cited

Anaka, M., C. D. MacDonald, E. Barkova, K. Simon, R. Rostom *et al.*, 2008 The white gene of Drosophila melanogaster encodes a protein with a role in courtship behavior. J. Neurogenet. 22: 243–276.

Bailey, T. L., N. Williams, C. Misleh, and W. W. Li, 2006 MEME: discovering and analyzing DNA and protein sequence motifs. Nucleic Acids Res. 34: W369–W373.

Barrandon, C., B. Spiluttini, and O. Bensaude, 2008 Non-coding RNAs regulating the transcriptional machinery. Biol. Cell 100: 83–95.

Biessmann, H., 1985 Molecular analysis of the yellow gene (y) region of Drosophila melanogaster. Proc. Natl. Acad. Sci. USA 82: 7369–7373.

Brock, H. W., J. W. Hodgson, S. Petruk, and A. Mazo, 2009 Regulatory noncoding RNAs at Hox loci. Biochem. Cell Biol. 87: 27–34.

Burge, C., and S. Karlin, 1997 Prediction of complete gene structures in human genomic DNA. J. Mol. Biol. 268: 78–94.
Bushati, N., A. Stark, J. Brennecke, and S. M. Cohen, 2008 Temporal reciprocity of miRNAs and their targets during the maternal-to-zygotic transition in Drosophila. Curr. Biol. 18: 501–506.
Campuzano, S., L. Carramolino, C. V. Cabrera, M. Ruiz-Gomez, R. Villares *et al.*, 1985 Molecular genetics of the achaete-scute gene complex of D. melanogaster. Cell 40: 327–338.
Campuzano, S., L. Balcells, R. Villares, L. Carramolino, L. Garcia-Alonso *et al.*, 1986 Excess function hairy-wing mutations caused by gypsy and copia insertions within structural genes of the achaete-scute locus of Drosophila. Cell 44: 303–312.
Chen, J. L., K. L. Huisinga, M. M. Viering, S. A. Ou, C. T. Wu *et al.*, 2002 Enhancer action in trans is permitted throughout the Drosophila genome. Proc. Natl. Acad. Sci. USA 99: 3723–3728.
Chen, L. L., and G. G. Carmichael, 2010 Decoding the function of nuclear long non-coding RNAs. Curr. Opin. Cell Biol. 22: 357–364.
Chia, W., G. Howes, M. Martin, Y. B. Meng, K. Moses *et al.*, 1986 Molecular analysis of the *yellow* locus of *Drosophila*. EMBO J. 5: 3597–3605.
Chopra, V. S., J. Cande, J. W. Hong, and M. Levine, 2009 Stalled Hox promoters as chromosomal boundaries. Genes Dev. 23: 1505–1509.
Cirelli, C., 2006 Sleep disruption, oxidative stress, and aging: new insights from fruit flies. Proc. Natl. Acad. Sci. USA 103: 13901–13902.
Cirelli, C., 2009 The genetic and molecular regulation of sleep: from fruit flies to humans. Nat. Rev. Neurosci. 10: 549–560.
Cirelli, C., and D. Bushey, 2008 Sleep and wakefulness in Drosophila melanogaster. Ann. N. Y. Acad. Sci. 1129: 323–329.
Cirelli, C., D. Bushey, S. Hill, R. Huber, R. Kreber *et al.*, 2005 Reduced sleep in Drosophila Shaker mutants. Nature 434: 1087–1092.
Clark, M. B., and J. S. Mattick, 2011 Long noncoding RNAs in cell biology. Semin. Cell Dev. Biol. (in press).
de Wit, E., and B. van Steensel, 2009 Chromatin domains in higher eukaryotes: insights from genome-wide mapping studies. Chromosoma 118: 25–36.
Deng, X., and V. H. Meller, 2006 Non-coding RNA in fly dosage compensation. Trends Biochem. Sci. 31: 526–532.
Drapeau, M. D., A. Radovic, P. J. Wittkopp, and A. D. Long, 2003 A gene necessary for normal male courtship, yellow, acts downstream of fruitless in the Drosophila melanogaster larval brain. J. Neurobiol. 55: 53–72.
Drapeau, M. D., S. A. Cyran, M. M. Viering, P. K. Geyer, and A. D. Long, 2006 A *cis*-regulatory sequence within the yellow locus of Drosophila melanogaster required for normal male mating success. Genetics 172: 1009–1030.
Galindo, M. I., J. I. Pueyo, S. Fouix, S. A. Bishop, and J. P. Couso, 2007 Peptides encoded by short ORFs control development and define a new eukaryotic gene family. PLoS Biol. 5: e106.
Garcia-Bellido, A., and J. F. de Celis, 2009 The complex tale of the achaete-scute complex: a paradigmatic case in the analysis of gene organization and function during development. Genetics 182: 631–639.
Garcia-Garcia, M. J., P. Ramain, P. Simpson, and J. Modolell, 1999 Different contributions of pannier and wingless to the patterning of the dorsal mesothorax of Drosophila. Development 126: 3523–3532.
Geyer, P. K., and V. G. Corces, 1987 Separate regulatory elements are responsible for the complex pattern of tissue-specific and developmental transcription of the *yellow* locus in *Drosophila melanogaster*. Genes Dev. 1: 996–1004.
Geyer, P. K., C. Spana, and V. G. Corces, 1986 On the molecular mechanism of gypsy-induced mutations at the yellow locus of Drosophila melanogaster. EMBO J. 5: 2657–2662.
Gibert, J. M., and P. Simpson, 2003 Evolution of cis-regulation of the proneural genes. Int. J. Dev. Biol. 47: 643–651.
Gong, W. J., and K. G. Golic, 2003 Ends-out, or replacement, gene targeting in *Drosophila*. Proc. Natl. Acad. Sci. USA 100: 2556–2561.
Gong, W. J., and K. G. Golic, 2004 Genomic deletions of the *Drosophila melanogaster* Hsp70 genes. Genetics 168: 1467–1476.
Graveley, B. R., A. N. Brooks, J. W. Carlson, M. O. Duff, J. M. Landolin *et al.*, 2011 The developmental transcriptome of Drosophila melanogaster. Nature 471: 473–479.
Hanyu-Nakamura, K., H. Sonobe-Nojima, A. Tanigawa, P. Lasko, and A. Nakamura, 2008 Drosophila Pgc protein inhibits P-TEFb recruitment to chromatin in primordial germ cells. Nature 451: 730–733.
Hashimoto, Y., T. Kondo, and Y. Kageyama, 2008 Lilliputians get into the limelight: novel class of small peptide genes in morphogenesis. Dev. Growth Differ. 50(Suppl 1): S269–S276.
Hendricks, J. C., S. M. Finn, K. A. Panckeri, J. Chavkin, J. A. Williams *et al.*, 2000 Rest in Drosophila is a sleep-like state. Neuron 25: 129–138.
Hendricks, J. C., S. Lu, K. Kume, J. C. Yin, Z. Yang *et al.*, 2003 Gender dimorphism in the role of cycle (BMAL1) in rest, rest regulation, and longevity in Drosophila melanogaster. J. Biol. Rhythms 18: 12–25.
Ho, K. S., and A. Sehgal, 2005 Drosophila melanogaster: an insect model for fundamental studies of sleep. Methods Enzymol. 393: 772–793.
Hurst, L. D., C. Pal, and M. J. Lercher, 2004 The evolutionary dynamics of eukaryotic gene order. Nat. Rev. Genet. 5: 299–310.
Ilik, I., and A. Akhtar, 2009 roX RNAs: non-coding regulators of the male X chromosome in flies. RNA Biol. 6: 113–121.
Inagaki, S., K. Numata, T. Kondo, M. Tomita, K. Yasuda *et al.*, 2005 Identification and expression analysis of putative mRNA-like non-coding RNA in Drosophila. Genes Cells 10: 1163–1173.
Jolly, C., and S. C. Lakhotia, 2006 Human sat III and Drosophila hsr omega transcripts: a common paradigm for regulation of nuclear RNA processing in stressed cells. Nucleic Acids Res. 34: 5508–5514.
Koh, K., J. M. Evans, J. C. Hendricks, and A. Sehgal, 2006 A *Drosophila* model for age-associated changes in sleep:wake cycles. Proc. Natl. Acad. Sci. USA 103: 13843–13847.
Kondo, T., Y. Hashimoto, K. Kato, S. Inagaki, S. Hayashi *et al.*, 2007 Small peptide regulators of actin-based cell morphogenesis encoded by a polycistronic mRNA. Nat. Cell Biol. 9: 660–665.
Koya, S. K., and V. H. Meller, 2011 roX RNAs and genome regulation in Drosophila melanogaster. Prog. Mol. Subcell. Biol. 51: 147–160.
Kozomara, A., and S. Griffiths-Jones, 2011 miRBase: integrating microRNA annotation and deep-sequencing data. Nucleic Acids Res. 39: D152–D157.
Kuhn, E. J., and P. K. Geyer, 2003 Genomic insulators: connecting properties to mechanism. Curr. Opin. Cell Biol. 15: 259–265.
Kume, K., S. Kume, S. K. Park, J. Hirsh, and F. R. Jackson, 2005 Dopamine is a regulator of arousal in the fruit fly. J. Neurosci. 25: 7377–7384.
Lee, J. M., and E. L. Sonnhammer, 2003 Genomic gene clustering analysis of pathways in eukaryotes. Genome Res. 13: 875–882.
Li, Z., M. Liu, L. Zhang, W. Zhang, G. Gao *et al.*, 2009 Detection of intergenic non-coding RNAs expressed in the main developmental stages in Drosophila melanogaster. Nucleic Acids Res. 37: 4308–4314.
Mallik, M., and S. C. Lakhotia, 2010 Improved activities of CREB binding protein, heterogeneous nuclear ribonucleoproteins and proteasome following downregulation of noncoding hsromega transcripts help suppress poly(Q) pathogenesis in fly models. Genetics 184: 927–945.

Markow, T. A., S. Beall, and L. M. Matzkin, 2009 Egg size, embryonic development time and ovoviviparity in Drosophila species. J. Evol. Biol. 22: 430–434.

Martens, J. A., L. Laprade, and F. Winston, 2004 Intergenic transcription is required to repress the Saccharomyces cerevisiae SER3 gene. Nature 429: 571–574.

Martianov, I., A. Ramadass, A. Serra Barros, N. Chow, and A. Akoulitchev, 2007 Repression of the human dihydrofolate reductase gene by a non-coding interfering transcript. Nature 445: 666–670.

Matouk, I. J., I. Abbasi, A. Hochberg, E. Galun, H. Dweik *et al.*, 2009 Highly upregulated in liver cancer noncoding RNA is overexpressed in hepatic colorectal metastasis. Eur. J. Gastroenterol. Hepatol. 21: 688–692.

Meller, V. H., and B. P. Rattner, 2002 The roX genes encode redundant male-specific lethal transcripts required for targeting of the MSL complex. EMBO J. 21: 1084–1091.

Mercer, T. R., M. E. Dinger, J. Mariani, K. S. Kosik, M. F. Mehler *et al.*, 2008 Noncoding RNAs in long-term memory formation. Neuroscientist 14: 434–445.

Mercer, T. R., M. E. Dinger, and J. S. Mattick, 2009 Long non-coding RNAs: insights into functions. Nat. Rev. Genet. 10: 155–159.

Modolell, J., and S. Campuzano, 1998 The achaete-scute complex as an integrating device. Int. J. Dev. Biol. 42: 275–282.

Mount, S. M., 1987 Sequence similarity. Nature 325: 487.

Nash, W. G., and R. J. Yarkin, 1974 Genetic regulation and pattern formation: a study of the yellow locus in Drosophila melanogaster. Genet. Res. 24: 19–26.

Negre, B., and P. Simpson, 2009 Evolution of the achaete-scute complex in insects: convergent duplication of proneural genes. Trends Genet. 25: 147–152.

Ogawa, Y., and J. T. Lee, 2002 Antisense regulation in X inactivation and autosomal imprinting. Cytogenet. Genome Res. 99: 59–65.

Panzitt, K., M. M. Tschernatsch, C. Guelly, T. Moustafa, M. Stradner *et al.*, 2007 Characterization of HULC, a novel gene with striking up-regulation in hepatocellular carcinoma, as noncoding RNA. Gastroenterology 132: 330–342.

Parnell, T. J., M. M. Viering, A. Skjesol, C. Helou, E. J. Kuhn *et al.*, 2003 An endogenous suppressor of hairy-wing insulator separates regulatory domains in Drosophila. Proc. Natl. Acad. Sci. USA 100: 13436–13441.

Parnell, T. J., E. J. Kuhn, B. L. Gilmore, C. Helou, M. S. Wold *et al.*, 2006 Identification of genomic sites that bind the Drosophila suppressor of Hairy-wing insulator protein. Mol. Cell. Biol. 26: 5983–5993.

Pepling, M., and S. M. Mount, 1990 Sequence of a cDNA from the Drosophila melanogaster white gene. Nucleic Acids Res. 18: 1633.

Petruk, S., Y. Sedkov, K. M. Riley, J. Hodgson, F. Schweisguth *et al.*, 2006 Transcription of bxd noncoding RNAs promoted by trithorax represses Ubx in cis by transcriptional interference. Cell 127: 1209–1221.

Pinto, B. S., S. R. Wilmington, E. E. Hornick, L. L. Wallrath, and P. K. Geyer, 2008 Tissue-specific defects are caused by loss of the drosophila MAN1 LEM domain protein. Genetics 180: 133–145.

Poliseno, L., L. Salmena, J. Zhang, B. Carver, W. J. Haveman *et al.*, 2010 A coding-independent function of gene and pseudogene mRNAs regulates tumour biology. Nature 465: 1033–1038.

Prasanth, K. V., and D. L. Spector, 2007 Eukaryotic regulatory RNAs: an answer to the 'genome complexity' conundrum. Genes Dev. 21: 11–42.

Prasanth, K. V., T. K. Rajendra, A. K. Lal, and S. C. Lakhotia, 2000 Omega speckles: a novel class of nuclear speckles containing hnRNPs associated with noncoding hsr-omega RNA in Drosophila. J. Cell Sci. 113(Pt 19): 3485–3497.

Raab, J. R., and R. T. Kamakaka, 2010 Insulators and promoters: closer than we think. Nat. Rev. Genet. 11: 439–446.

Romani, S., S. Campuzano, and J. Modolell, 1987 The achaete-scute complex is expressed in neurogenic regions of Drosophila embryos. EMBO J. 6: 2085–2092.

Rusinov, V., V. Baev, I. N. Minkov, and M. Tabler, 2005 MicroInspector: a web tool for detection of miRNA binding sites in an RNA sequence. Nucleic Acids Res. 33: W696–W700.

Schwartz, S., Z. Zhang, K. A. Frazer, A. Smit, C. Riemer *et al.*, 2000 PipMaker—a web server for aligning two genomic DNA sequences. Genome Res. 10: 577–586.

Sehgal, A., W. Joiner, A. Crocker, K. Koh, S. Sathyanarayanan *et al.*, 2007 Molecular analysis of sleep: wake cycles in Drosophila. Cold Spring Harb. Symp. Quant. Biol. 72: 557–564.

Shaw, P. J., C. Cirelli, R. J. Greenspan, and G. Tononi, 2000 Correlates of sleep and waking in Drosophila melanogaster. Science 287: 1834–1837.

Soshnev, A. A., X. Li, M. D. Wehling, and P. K. Geyer, 2008 Context differences reveal insulator and activator functions of a Su(Hw) binding region. PLoS Genet. 4: e1000159.

Stark, A., M. F. Lin, P. Kheradpour, J. S. Pedersen, L. Parts *et al.*, 2007 Discovery of functional elements in 12 Drosophila genomes using evolutionary signatures. Nature 450: 219–232.

Taft, R. J., K. C. Pang, T. R. Mercer, M. Dinger, and J. S. Mattick, 2010 Non-coding RNAs: regulators of disease. J. Pathol. 220: 126–139.

Tautz, D., and C. Pfeifle, 1989 A non-radioactive in situ hybridization method for the localization of specific RNAs in Drosophila embryos reveals translational control of the segmentation gene hunchback. Chromosoma 98: 81–85.

Thomsen, S., S. Anders, S. C. Janga, W. Huber, and C. R. Alonso, 2010 Genome-wide analysis of mRNA decay patterns during early Drosophila development. Genome Biol. 11: R93.

Timinszky, G., M. Bortfeld, and A. G. Ladurner, 2008 Repression of RNA polymerase II transcription by a Drosophila oligopeptide. PLoS ONE 3: e2506.

Tsurudome, K., K. Tsang, E. H. Liao, R. Ball, J. Penney *et al.*, 2010 The Drosophila miR-310 cluster negatively regulates synaptic strength at the neuromuscular junction. Neuron 68: 879–893.

Tupy, J. L., A. M. Bailey, G. Dailey, M. Evans-Holm, C. W. Siebel *et al.*, 2005 Identification of putative noncoding polyadenylated transcripts in *Drosophila melanogaster*. Proc. Natl. Acad. Sci. USA 102: 5495–5500.

Walter, M. F., B. C. Black, G. Afshar, A. Y. Kermabon, T. R. Wright *et al.*, 1991 Temporal and spatial expression of the yellow gene in correlation with cuticle formation and dopa decarboxylase activity in Drosophila development. Dev. Biol. 147: 32–45.

Wang, J., X. Liu, H. Wu, P. Ni, Z. Gu *et al.*, 2010 CREB up-regulates long non-coding RNA, HULC expression through interaction with microRNA-372 in liver cancer. Nucleic Acids Res. 38: 5366–5383.

Willingham, A. T., S. Dike, J. Cheng, J. R. Manak, I. Bell *et al.*, 2006 Transcriptional landscape of the human and fly genomes: nonlinear and multifunctional modular model of transcriptomes. Cold Spring Harb. Symp. Quant. Biol. 71: 101–110.

Yi, G., S. H. Sze, and M. R. Thon, 2007 Identifying clusters of functionally related genes in genomes. Bioinformatics 23: 1053–1060.

Yuan, Q., W. J. Joiner, and A. Sehgal, 2006 A sleep-promoting role for the Drosophila serotonin receptor 1A. Curr. Biol. 16: 1051–1062.

Zhang, S. D., and W. F. Odenwald, 1995 Misexpression of the white (w) gene triggers male-male courtship in *Drosophila*. Proc. Natl. Acad. Sci. USA 92: 5525–5529.

Zuker, M., 2003 Mfold web server for nucleic acid folding and hybridization prediction. Nucleic Acids Res. 31: 3406–3415.

Communicating editor: J. A. Birchler

GENETICS

Supporting Information
http://www.genetics.org/content/suppl/2011/07/20/genetics.111.131706.DC1

A Conserved Long Noncoding RNA Affects Sleep Behavior in *Drosophila*

Alexey A. Soshnev, Hiroshi Ishimoto, Bryant F. McAllister, Xingguo Li, Misty D. Wehling, Toshihiro Kitamoto, and Pamela K. Geyer

DOI: 10.1534/genetics.111.131706

Motif 1.1 (yarP)

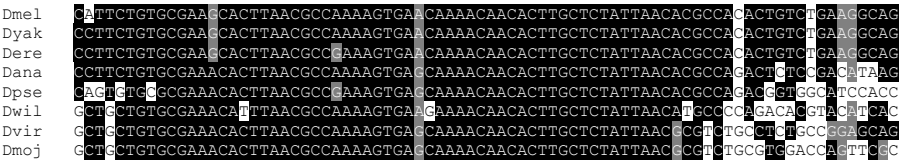

Motif 1.2

Motif 1.3

Motif 1.4

Motif 2.1

Motif 2.3

Motif 2.4

Motif 2.5

Figure S1 Multiple conserved MEME-identified motifs identified in the y-ac intergenic region. Comparative sequence analyses were completed using the y-ac intergenic regions from nine Drosophila species. These include species in the subgenus Sophophora estimated to represent 10 million years (myrs) of evolution [D. yakuba (yak), D. erecta (ere)], and 20-30 myrs [D. ananassae (ana), D. pseudoobscura (pse), D. willistoni (wil)], and species in the subgenus Drosophila estimated to represent 40-60 myrs of evolution [D. virilis (vir) , D. mojavensis (moj), and D. grimshawi (gri)]. ClustalW2 (http://www.ebi.ac.uk/Tools/msa/clustalw2) and BoxShade (http://www.ch.embnet.org/software/BOX_form.html) were used to show identity (black) or similarity in base (purine or pyrimidine, grey). Gaps in the alignments are shown by (-).

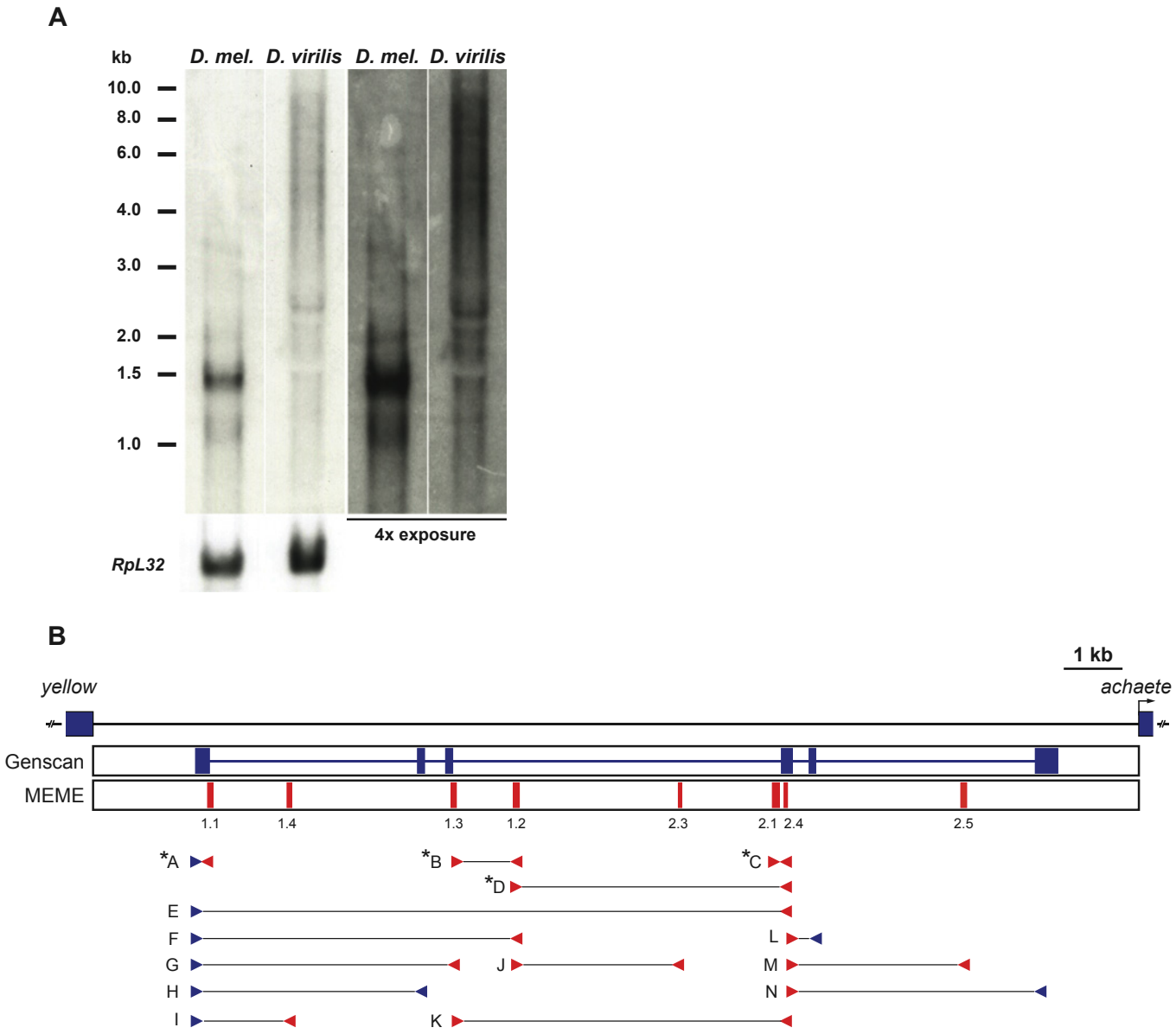

Figure S2 RNA analyses of D. virilis and D. melanogaster yar. A. Northern analysis of Poly A+ RNA from 6-12 hour D. melanogaster Canton S embryos (3.5 µg) or 16-24 hour D. virilis embryos (10 µg) hybridized with 32P-dATP- labeled DNA probes corresponding to D. melanogaster yar isoform containing exons 1, 3 and 4 (Genbank GQ329854) or D. virilis yar cDNA B. RpL32 is a constitutively expressed gene that served as a loading control. The far right panels show the same blots exposed four times longer. B: Strategy for analysis of intergenic transcription in D. virilis. Top, structure of the y-ac intergenic region in D. virilis, showing the location of the Genscan-predicted gene (blue) and MEME-identified conserved motifs (red). Bottom, schematic of the strategies used for PCR analyses of RNAs isolated from 16-24 hr D. virilis embryos using the indicated primer pairs. This developmental time was chosen, as it represents the period of maximal expression of the yar gene (Figure 2). Primers were anchored in Genscan-predicted exons (blue arrowheads) and MEME-identified motifs (red arrowheads). As a positive control, all primer pairs were tested with D. virilis genomic DNA, and each yielded products of expected size. Only primer pairs shown in A, B, C and D yielded products when embryonic cDNAs were used as a template. These are indicated by asterisks (*).

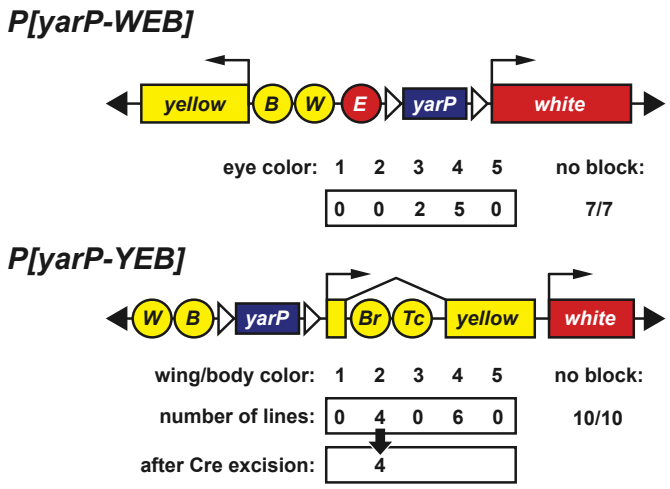

Figure S3 The yar promoter (yarP) does not act as enhancer blocker in transgene assays. Two enhancer blocking reporter transposons were tested. In P[yarP-white enhancer blocking (WEB)], the enhancer blocking w reporter gene carried yarP inserted between direct repeats of loxP sites (white arrowheads), positioned either between the eye enhancer (E) and w promoter. In P[yarP-WEB], the y gene was used as a transformation marker. In P[YEB], the enhancer blocking y reporter gene carried yarP inserted between the wing (W) and body (B) enhancers and promoter of the y gene, which also carried the downstream bristle (Br) and tarsal claw (Tc) enhancers. Eye pigmentation was scored in seven transgenic P[WEB] lines, where 1 represents white eyes and 5 represents red pigmentation. In all lines, high levels of pigmentation were found (scores of 3, 4), implying no block of the w eye enhancer (no block). Cuticle pigmentation in ten transgenic P[YEB] lines was scored, where 1 represents light yellow color of a null and 5 represents black pigmentation of wild type flies. In six lines, dark pigmentation (scores of 4 wing, 4 body) was found. In four lines, light pigmentation (scores of 2 wing, 2 body) was observed. Lines established from these four lines that lacked yarP alos showed light pigmentation (bottom arrow), indicating no block of the y enhancers.

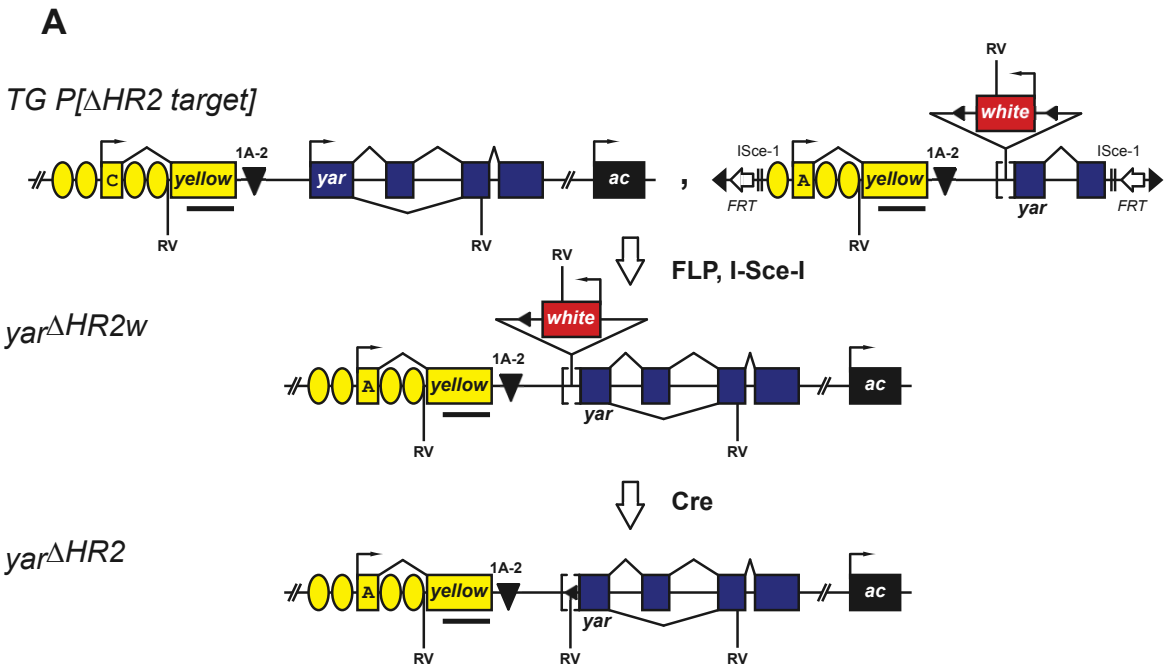
A
TG P[ΔHR2 target]
C
yellow
1A-2
yar
ac
RV
ISce-1
FRT
A
white
yar
yarΔHR2w
FLP, I-Sce-I
yarΔHR2
Cre

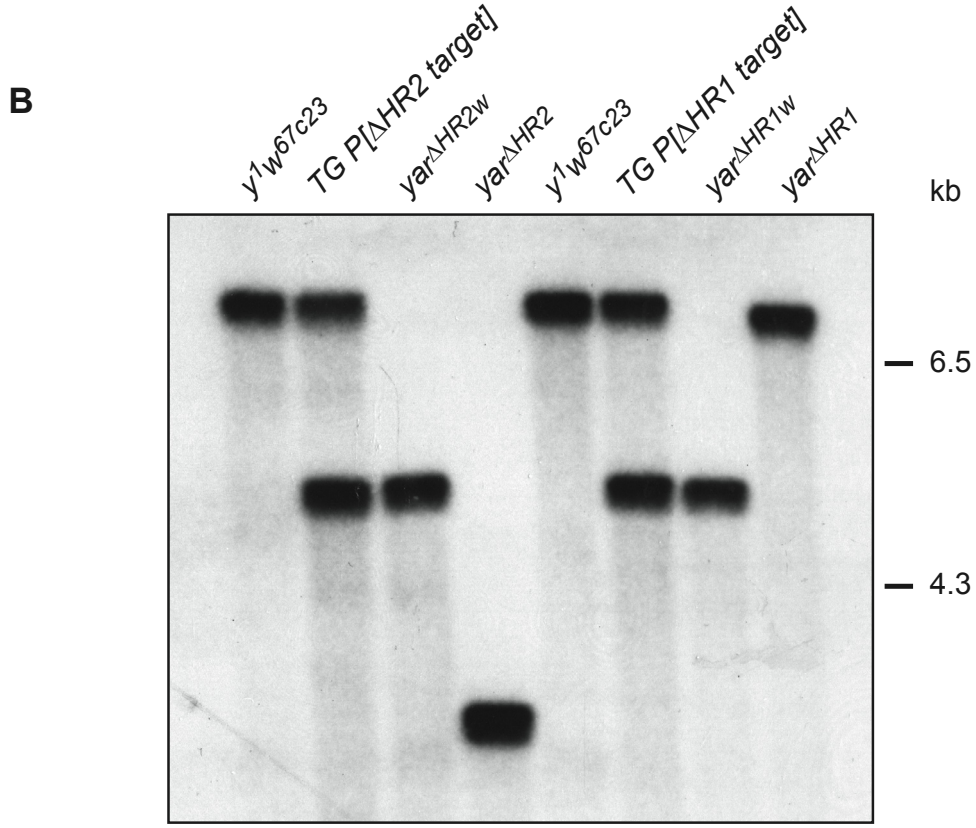
B
y1w67c23
TG P[ΔHR2 target]
yarΔHR2w
yarΔHR2
y1w67c23
TG P[ΔHR1 target]
yarΔHR1w
yarΔHR1
kb
6.5
4.3

Figure S4 Generation and of yar homologous recombinant deletion lines. A: Ends-out targeting strategy to remove yar promoter. The targeting transposon P[ΔHR2 target] was injected into y1 mutant background, which has a mutation in the y translation start site (ATG to CTG). The P[ΔHR2 target] transposon carries a y gene that encodes a wild-type RNA, but lacks the wing enhancer. The sequences encompassing the yar promoter are replaced by w gene flanked by LoxP sites (small black triangles). The FRT sites (white arrows) and ISce-1 sites (double dashes) are flanking the targeting construct. Transgenic flies carrying the P[ΔHR2 target] had dark body, light wings and orange eyes. FLP and ISce-1 enzymes catalyzed the replacement of the y1 allele at the endogenous location, and the yar promoter was substituted by w gene. The recombinant flies had dark body, dark wings and red eyes. Cre recombinase was used to remove the w gene, leaving behind a loxP site. Black bar indicates the y ClaI-BglII fragment used as a probe in Southern analyses below. EcoRV restriction enzyme cut sites are indicated. In yarΔHR2, a novel EcoRV cut site was introduced after Cre excision of w gene. B: Southern analysis of the yar genomic region. Genomic DNA isolated from ten flies was digested with EcoRV and resolved on agarose gel. DNAs were transferred to Nytran membrane and hybridized with a 32P-dATP-labeled probe made with ClaI to BglII fragment of y gene, which recognizes an endogenous band of 7.6 kb in and transgene band of 4.5 kb.

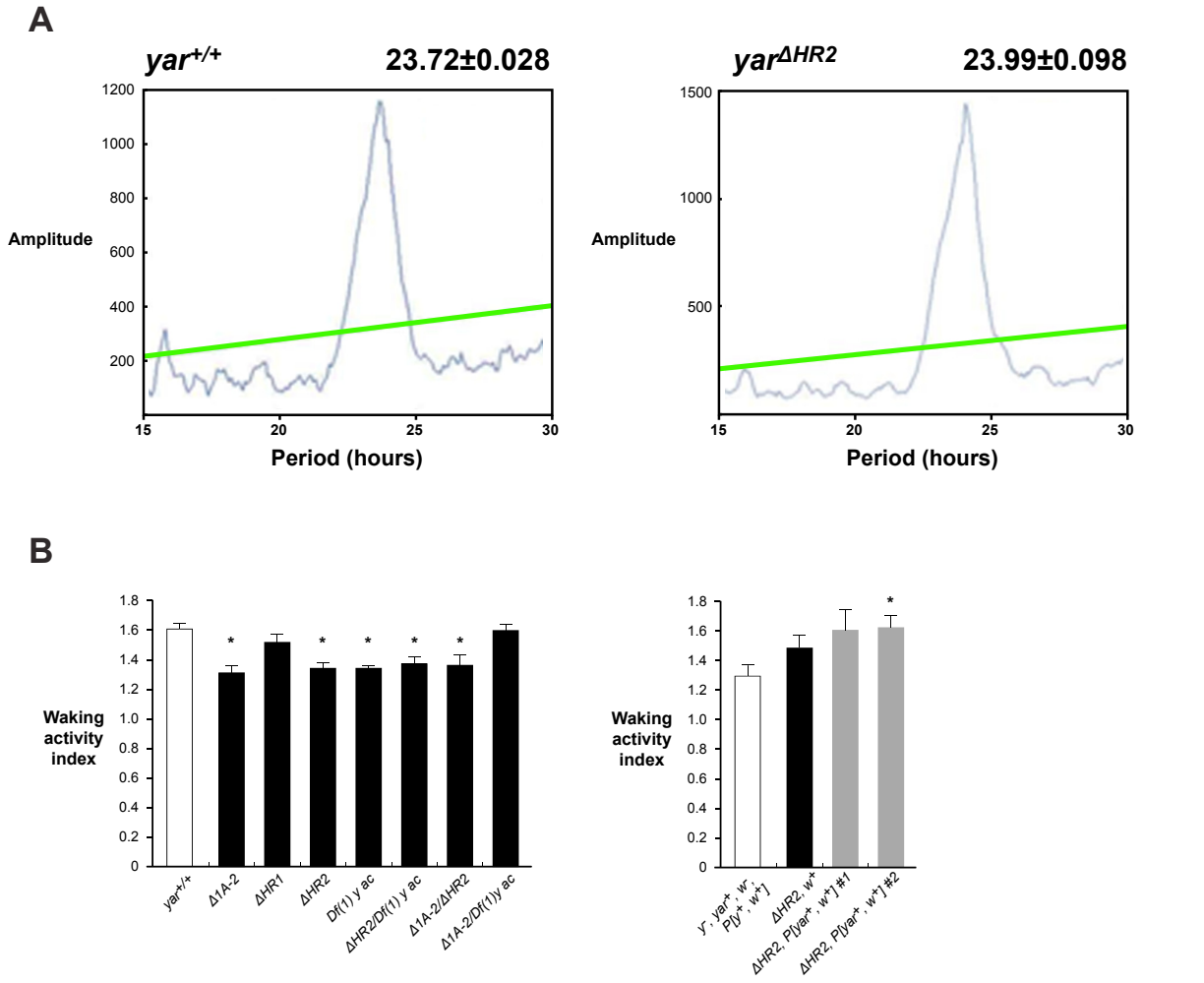

Figure S5 Sleep analyses of yar mutants. A. Analysis of circadian rhythm. Shown is the locomotor activity of females from the reference yar+/+ (y1 yar+ w67c23, white bar) and the yar mutant (y1 yarΔHR2 w67c23) line kept in constant dark for ten days, after being reared for three days under twelve hr light/ twelve hr dark conditions. Circadian periodicity was calculated using the autocorrelation function of ClockLab software (Actimetrics at http://www.actimetrics.com/). The autocorrelation analysis shows that both strains maintain normal circadian rythmicity under this free running condition. The average periods for reference and yarΔHR2 were 23.72 and 23.99 hrs, respectively. B. Analysis of waking activity. Waking activity index in the reference yar+/+ (y1 yar+ w67c23, white bar) line and yar mutant lines (black bars) is calculated as a ratio of activity counts per waking time. Introduction of P[yar w] does not reduce the waking activity in rescued yar mutants. Kruskal-Wallis one way ANOVA, *, P<0.005.

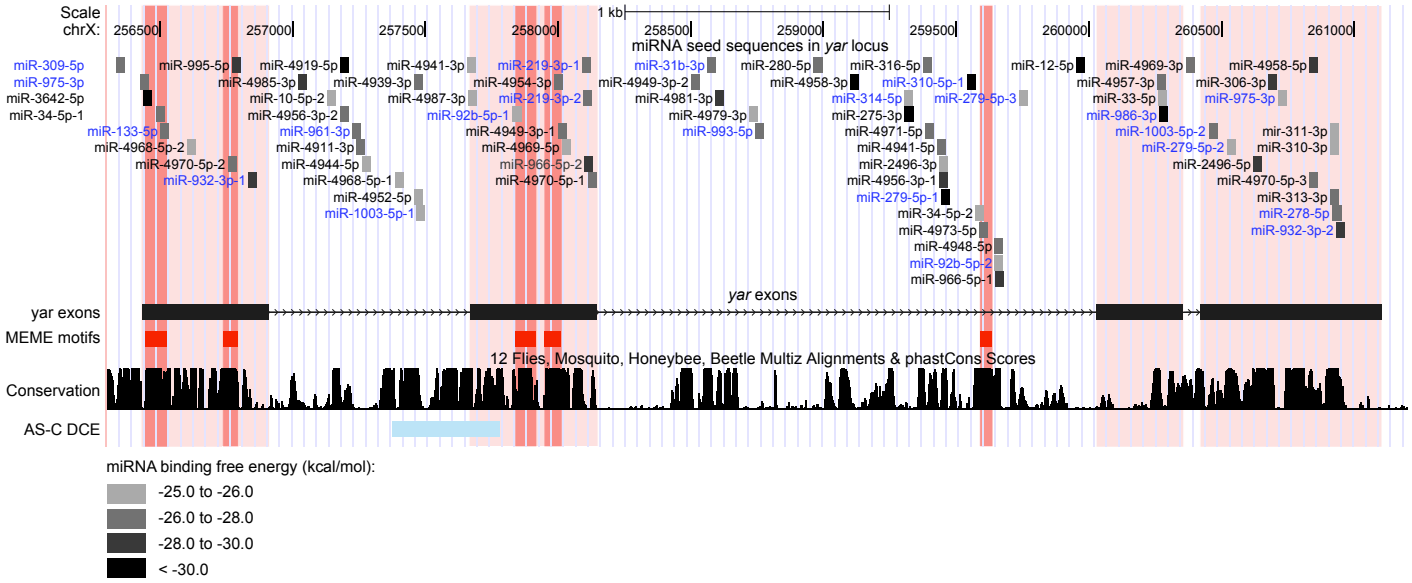

Figure S6 Predicted miRNA seed sequences in the yar gene. Show is the UCSC Genome Browser view of yar genomic region with predicted seed sequences corresponding to the experimentally identified (black) and predicted (blue) D. melanogaster miRNAs (miRBase release 17). Boxes representing seed sequences are colored based on free energy of miRNA-yar interaction, with strongest seeds (<-30 kcal/mol) colored black and weaker seeds colored in lighter gray. High free energy cutoff for these analyses was set at -25 kcal/mol. The position of the Dorsocentral enhancer of AS-C complex genes is indicated by light blue bar.

Table S1 Primers

***Drosophila melanogaster* primers**		
yar.spliced.Fw	AGA-CGC-CCT-TTA-ATT-TCA-CGC-TGC	amplify spliced *yar* (Fig.1C)
yar.spliced.Rev	TCC-GTC-TGC-CTT-TGT-GTT-TAG-ACG	
yar.intron.Fw	GCT-CCG-TAT-TCC-ACT-TCT-CTG-AGG	amplify *yar* intron (Fig.1C)
yar.intron.Rev	GAT-TGC-GTG-TGC-CTC-GTG-TGC-TG	
Ras64B.spliced.Fw	GGC-AAG-TCA-GCG-ATA-ACG-ATA-CAG-TTC	amplify spliced *Ras64B* (Fig.1C)
Ras64B.spliced.Rev	CGA-GTC-TTC-AAT-GGT-GGG-ATC-GTA-GTC	
Ras64B.intron.Fw	AAT-CAT-CAT-CAT-CAT-CAT-CAT-TGG-CAG	amplify *Ras64B* intron (Fig.1C)
Ras64B.intron.Rev	ATA-TAC-ACG-AAA-GAT-GTG-CAG-ATG-ACG	
yar.genomic.Fw	CGG-ATC-CAA-GGT-TAA-GAG-TTT-ACG-C	amplify *yar* genomic region to generate rescue
yar.genomic.Rev	CGG-ATC-CTA-ATT-TCA-ATG-CCG-TAT-CAT-C	construct, contain BamHI cut sites (Fig. 3)
yellow.Fw	TGG-AGT-CGA-ACA-CTT-TGG-CAA-TCG-G	amplify *yellow* (Fig.4)
yellow.Rev	CCC-ACA-GCC-GAC-CAC-ACT-CAT	
yar.Fw	GTA-TAT-CCA-CAT-CAC-CAG-ACC-TCA-GGA-C	amplify *yar* (Fig.4)
yar.Rev	ACA-TCC-TCG-AAT-CAC-TAT-GCA-AGT-CG	
achaete.Fw	CTT-CGG-CCT-TTA-ATG-GAC-CCT-CTG-TT	amplify *achaete* (Fig.4)
achaete.Rev	AAT-CGT-CGA-TGT-TGC-TGG-CTT-GC	
scute.Fw	CTA-TCG-CCT-GGT-TCC-TCG-CC	amplify *scute* (Fig.4)
scute.Rev	TCC-ACC-AGA-TCC-TGA-AGC-CTC-C	
RpL32.Fw	AAG-ATG-ACC-ATC-CGC-CCA-GCA-TAC	amplify *RpL32* (housekeeping gene
RpL32.Rev	ACG-CAC-TCT-GTT-GTC-GAT-ACC-CTT-G	control (Fig.4)
Ras64B.Fw	AGG-AAG-TGC-TGC-CTG-ATG-TAG-AAG	amplify *Ras64B* (housekeeping gene
Ras64B.Rev	TTA-TAT-GTT-GGC-TCC-TGC-TTC-CGC	control (Fig.4)
***Drosophila virilis* primers**		
Dvir.achaete.Fw	GCA-CGA-ATT-GTT-GGG-ATA-ATC-TTC	amplify *D. virilis achaete* (Fig.2)
Dvir.achaete.Rev	AAC-GCC-TCC-AAC-TCC-AGC-AGC	
Dvir.yellow.Fw	AAT-AGG-CAA-CAG-CAT-CAT-CGC-AGC	amplify *D. virilis yellow* (Fig.2)
Dvir.yellow.Rev	TTT-GAT-CTG-ACC-ACA-AAC-ACA-AGA-AT	
Dvir.RpL32.Fw	AGC-TCA-CGC-ACA-TTG-TGT-ACG-AGG	amplify *D. virilis RpL32* (Fig.2)
Dvir.RpL32.Rev	ACA-GAG-TGC-GTC-GTC-GCT-TCA-AG	
Dvir.RpL32-CDS.Fw	TGA-GAA-CGC-AGA-CGA-CCG-TTG-G	amplify *D. virilis RpL32* cDNA (used to
Dvir.RpL32-CDS.Rev	CAC-CAA-AAT-GAC-CAT-TCG-TCC-AGC	make probe in Suppl.Fig.2A)
Dvir.GS-ex1.Fw[A]	AAG-GCG-AAA-GCA-ACA-GCA-GCA-GC	amplify fragments of *D. virilis y-ac*
Dvir.1-3.Fw[B]	TCC-ACT-TGC-CAG-GTG-AGA-ATT-GAC	intergenic region (Fig.2, Suppl.Fig.2B).
Dvir.1-2.Fw[D]	GAG-CAC-ACT-TTT-GCC-TGC-GGT	Primer pairs that generated cDNAs A, B,
Dvir.2-1.Fw[C]	TCG-TTG-TGG-TTG-TCA-TTA-GTC-CGC-TG	C and D are indicated.
Dvir.2-4.Fw	GAT-CGT-GAG-TGC-CAG-AAG-CTG	
Dvir.1-1.Rev[A]	CTT-TTG-GCG-TTA-AGT-GTT-TCG	

Dvir.1-4.Rev	CAG-CTT-GAT-ATT-AAC-GCC-GTC-TAG
Dvir.GS-ex2.Rev	TTC-ACG-CGT-GTC-TTG-TCA-TAT-CGC-CAG-G
Dvir.1-3.Rev	GTC-AAT-TCT-CAC-CTG-GCA-AGT-GGA
Dvir.1-2.Rev[B]	ACC-GCA-GGC-AAA-AGT-GTG-CTC
Dvir.2-3.Rev	TTC-TCA-TTG-ATT-AAT-TGC-CAT-CAT-TAG-C
Dvir.2-4.Rev[C,D]	CAG-CTT-CTG-GCA-CTC-ACG-ATC
Dvir.GS-ex5.Rev	TCT-TCG-ACA-AGG-GTC-GCT-CTT-GGC-AG
Dvir.2-5.Rev	GCA-GCA-GGC-GCT-ATC-ATT-ATC-TGA-CAC
Dvir.GS-ex6.Rev	GCA-ATA-GAA-ATT-CGC-TCT-GGG-GTG-AAG-G

Table S2 Comparison of MEME-identified motifs between *D. melanogaster* and *D. virilis*

Motif	Position[1]	Length (nt)	Identity (%)	E-value
1.1[2]	256444	80	78.75	1.3e-140
1.4	256736	58	74.14	2.4e-069
1.3	257840	76	73.68	6.5e-107
1.2	257944	69	73.91	2.3e-120
2.3	259291	44	95.45	3.3e-107
2.1	261247	111	70.54	7.2e-222
2.4	261433	40	97.56	6.8e-103
2.5	262084	79	48.10	8.2e-107

[1]Indicates position of the first nucleotide in *D. melanogaster* genome (dm3, chrX)
[2]Encompasses *yar* promoter with two transcription start sites

Table S3

Table S3 is available for download as an Excel file at
http://www.genetics.org/content/suppl/2011/07/20/genetics.111.131706.DC1.